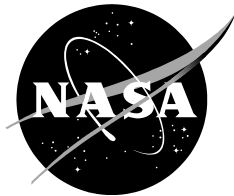


NASA/TM—2016-218850



Lateral Cutoff Analysis and Results from NASA's Farfield Investigation of No-Boom Thresholds

*Larry J. Cliatt II, Edward A. Haering Jr., Sarah R. Arnac, and Michael A. Hill
Armstrong Flight Research Center, Edwards, California*

February 2016

NASA STI Program ... in Profile

Since its founding, NASA has been dedicated to the advancement of aeronautics and space science. The NASA scientific and technical information (STI) program plays a key part in helping NASA maintain this important role.

The NASA STI program operates under the auspices of the Agency Chief Information Officer. It collects, organizes, provides for archiving, and disseminates NASA's STI. The NASA STI program provides access to the NTRS Registered and its public interface, the NASA Technical Reports Server, thus providing one of the largest collections of aeronautical and space science STI in the world. Results are published in both non-NASA channels and by NASA in the NASA STI Report Series, which includes the following report types:

- **TECHNICAL PUBLICATION.** Reports of completed research or a major significant phase of research that present the results of NASA Programs and include extensive data or theoretical analysis. Includes compilations of significant scientific and technical data and information deemed to be of continuing reference value. NASA counterpart of peer-reviewed formal professional papers but has less stringent limitations on manuscript length and extent of graphic presentations.
- **TECHNICAL MEMORANDUM.** Scientific and technical findings that are preliminary or of specialized interest, e.g., quick release reports, working papers, and bibliographies that contain minimal annotation. Does not contain extensive analysis.
- **CONTRACTOR REPORT.** Scientific and technical findings by NASA-sponsored contractors and grantees.

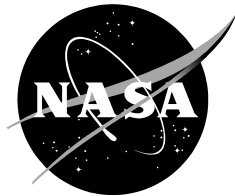
- **CONFERENCE PUBLICATION.** Collected papers from scientific and technical conferences, symposia, seminars, or other meetings sponsored or co-sponsored by NASA.
- **SPECIAL PUBLICATION.** Scientific, technical, or historical information from NASA programs, projects, and missions, often concerned with subjects having substantial public interest.
- **TECHNICAL TRANSLATION.** English-language translations of foreign scientific and technical material pertinent to NASA's mission.

Specialized services also include organizing and publishing research results, distributing specialized research announcements and feeds, providing information desk and personal search support, and enabling data exchange services.

For more information about the NASA STI program, see the following:

- Access the NASA STI program home page at <http://www.sti.nasa.gov>
- E-mail your question to help@sti.nasa.gov
- Phone the NASA STI Information Desk at 757-864-9658
- Write to:
NASA STI Information Desk
Mail Stop 148
NASA Langley Research Center
Hampton, VA 23681-2199

NASA/TM—2016-218850



Lateral Cutoff Analysis and Results from NASA's Farfield Investigation of No-Boom Thresholds

*Larry J. Cliatt II, Edward A. Haering Jr., Sarah R. Arnac, and Michael A. Hill
Armstrong Flight Research Center, Edwards, California*

National Aeronautics and
Space Administration

*Armstrong Flight Research Center
Edwards, California, 93523-0273*

February 2016

**NASA STI Support Services
Mail Stop 148
NASA Langley Research Center
Hampton, VA 23681-2199
757-864-9658**

**National Technical Information Service
5301 Shawnee Rd.
Alexandria, VA 22312
webmail@ntis.gov
703-605-6000**

Abstract

In support of the ongoing effort by the National Aeronautics and Space Administration (NASA) to bring supersonic commercial travel to the public, the NASA Armstrong Flight Research Center (AFRC) and the NASA Langley Research Center (LaRC), in partnership with other industry organizations and academia, conducted a flight research experiment to analyze acoustic propagation at the lateral edge of the sonic boom carpet. The name of the effort was the Farfield Investigation of No-boom Thresholds (FaINT). The test helped to build a dataset that will go toward further understanding of the unique acoustic propagation characteristics near the sonic boom carpet extremity. The FaINT was an effort that collected finely-space sonic boom data across the entire lateral cutoff transition region.

A major objective of the effort was to investigate the acoustic phenomena that occur at the audible edge of a sonic boom carpet, including the transition and shadow zones. A NASA F-18B aircraft made supersonic passes such that its sonic boom carpet transition zone would intersect a linear 60-microphone, 7500-ft long array. A TG-14 motor glider equipped with a microphone on its wing also attempted to capture the same sonic boom rays that were measured on the ground, at altitudes of 3000 – 6000 ft above ground level.

This paper determined an appropriate metric for sonic boom waveforms in the transition and shadow zones called Perceived Sound Exposure Level, and established a value of 65 dB as a limit for the acoustic levels defining the lateral extent of a sonic boom's noise region; analyzed the change in sonic boom levels as a function of distance from flight path both on the ground and 4500 ft above the ground; and compared between sonic boom measurements and numerical predictions.

Nomenclature

AAMP	Airborne Acoustic Measurement Platform
AFRC	Armstrong Flight Research Center
ANSI	American National Standards Institute
ASEL	A-weighted sound exposure level
B&K	Brüel & Kjær
BEAR	Boom Event Analyzer Recorder
BNC	Bayonet Neill-Concelman
BREN	Bare Reactor Experiment, Nevada
CSEL	C-weighted Sound Exposure Level
dB	decibels
ΔP	overpressure
FaINT	Farfield Investigation of No-boom Thresholds
ft	feet
GPS	global positioning system
Hp	pressure altitude
IRIG	inter-range instrumentation group time code
ISO	International Organization of Standards
km	kilometer
LAF	A-weighted exponential-time-averaged sound level (fast)
LAS	A-weighted exponential-time-averaged sound level (slow)

LCO	lateral cutoff
LDS	Ling Dynamic Systems
LNTE	Lossy Nonlinear Tricomi Equation
ms	milliseconds
NASA	National Aeronautics and Space Administration
nm	nautical mile
PL ₇₀	Stevens Mark VII Perceived Level
PL _{SEL}	Perceived Sound Exposure Level
RMS	root-mean-squared
SEL	sound exposure level
VDC	voltage in direct current

Introduction

Lateral cutoff occurs at the sonic boom carpet edge when the rays no longer reach the ground. Atmospheric effects – predominately the change in temperature with altitude – causes sonic boom rays to refract as they propagate to the ground. As air temperature increases toward the ground, the speed of sound increases, causing rays to propagate faster. This change in propagation speed results in a refracted path that becomes increasingly parallel to the ground. In raytracing terms used by computer models like PCBoom (ref. 1), sonic booms propagate at different azimuths (phi angles) from the airplane. 0-degree phi is directly below the airplane, and +/- 90-degrees phi is projected from either wing. Rays that propagate further distances spend more time in the atmosphere and, therefore, have greater refraction. As the magnitude of phi increases, eventually rays no longer reach the ground. Figure 1 shows the normalized predicted lateral sonic boom profile for an F-18 airplane at Mach 1.255, 36750 ft Hp, the median FaINT flight condition. The prediction was computed using PCBoom and U.S. Standard Atmospheric (ref. 2) conditions. It should be noted that the predicted pressure levels do not gradually decrease to zero; instead they abruptly end when the rays no longer reach the ground. The FaINT intended to investigate what actually occurs at this lateral cutoff and the region beyond, called the “shadow zone” (ref. 3).

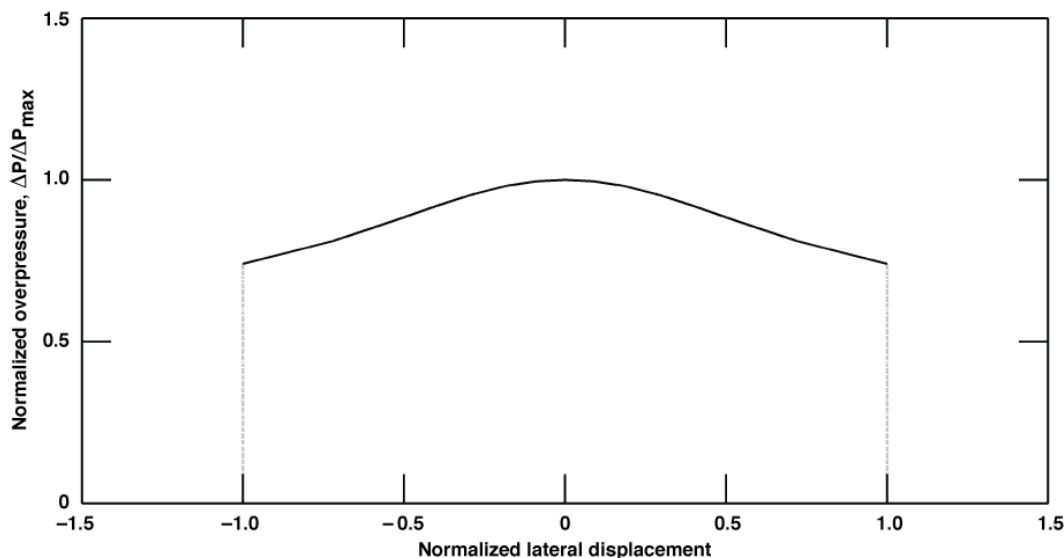


Figure 1. PCBoom-predicted lateral sonic boom profile. Mach 1.255, 36750 ft Hp.

Background

The primary sonic boom carpet, which is generated when the shockwaves directly underneath an airplane in supersonic flight intersect the ground, is only one component of acoustic disturbances classified as sonic booms. While some of these components, such as over-the-top and focused sonic booms, have garnered attention in the past and/or considerable research (refs. 4-6), sonic booms in the shadow zone (the area beyond the sonic boom carpet where geometrical acoustics predicts no signal) have been challenging to analyze due to their complex propagation (ref. 7). Figure 2 illustrates the extent of a sonic boom carpet envelope, while figure 3 depicts the most lateral rays that reach the ground in the primary sonic boom carpet. The latter shows a notional transition region, the lateral cutoff and shadow zone.

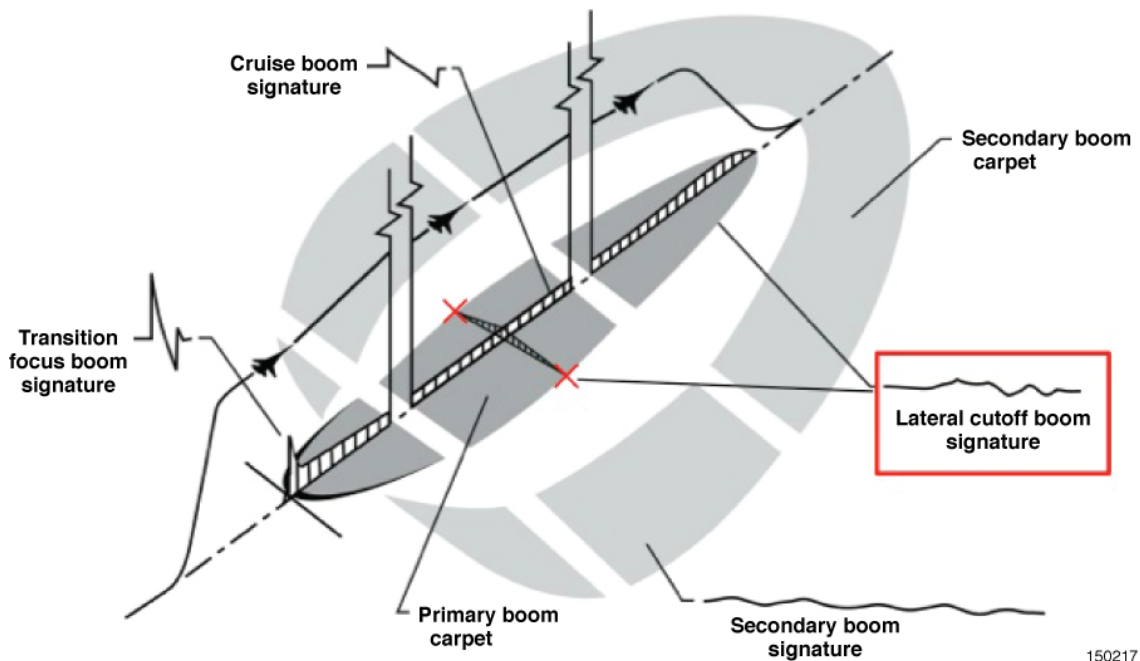


Figure 2. Sonic boom envelope.³

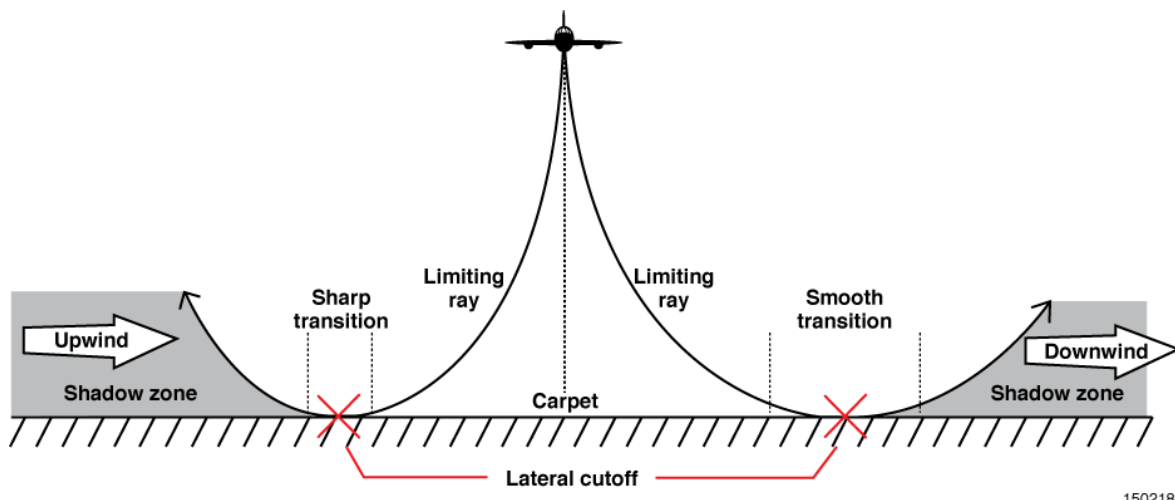


Figure 3. Sonic boom lateral cutoff, transition region, and shadow zone.¹⁸

The FaINT attempted to analyze these regions, where sonic boom carpet pressure signatures are transitioned into evanescent waves (sound waves that attenuate exponentially), as shown in figure 4. Distances noted are nautical miles (nm) laterally from the centerline flight path. Note the pressure axes on the left graph change scale with each microphone. The top pressure signature in the figure is within the sonic boom carpet, while the bottom pressure signature is most likely in the shadow zone. It can be seen that pressure signatures within the sonic boom carpet are traditional N-waves, but with increasing distance laterally beyond the sonic boom carpet, they attenuate in amplitude while increasing in length.

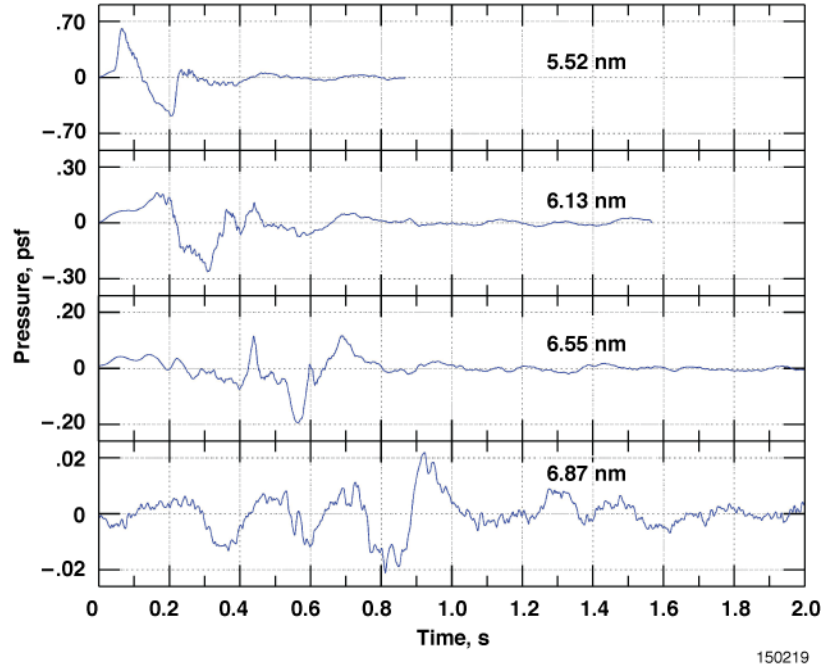


Figure 4. Example of sonic boom pressure signatures laterally across the transition region.

The key goals of the FaINT lateral cutoff missions were to develop and execute the methods to measure shadow zone acoustics at the edge of the sonic boom carpet, and to collect a comprehensive database of the resulting evanescent waves.

The FaINT test was a NASA collaborative effort with several industry partners. It was planned and managed out of the NASA Armstrong Flight Research Center (AFRC), while NASA Langley Research Center (LaRC) and Wyle (El Segundo, California) provided acoustic propagation expertise. Other partners included The Boeing Company (Chicago, Illinois); Gulfstream Aerospace Corporation (Savannah, Georgia); The Cessna Aircraft Company (Wichita, Kansas); The Pennsylvania State University (University Park, Pennsylvania); The Japan Aerospace Exploration Agency (Chōfu, Tokyo, Japan) and Dassault Aviation (Paris, France) – all of which provided invaluable instrumentation and sonic boom field operations proficiency.

Examining acoustic propagation at the lateral edge of the sonic boom carpet will help the aerospace industry understand the full extent and ranges of noises generated by a supersonic aircraft. Considerable sound levels can be experienced far beyond the sonic boom carpet predicted by computer models due to the difficulty in accurately modeling the evolution of sonic boom signatures within the sonic boom carpet to the evanescent waves that propagate into the shadow zone (fig. 4). Understanding the entire noise region caused by supersonic airplanes will be critical in determining target flight profiles and airplane designs for future commercial supersonic airplanes.

This paper focuses on quantifying the lateral extent of noise beyond a sonic boom's carpet; analyzing the change in sonic boom levels as a function of distance from flight path, using appropriate metrics for transition and shadow zone pressure signatures; changes in sound levels near lateral cutoff from the midfield to the ground; and comparisons between sonic boom measurements and numerical predictions. Two notable previous research efforts that included lateral cutoff measurement and analysis are the 1970 Bare Reactor Experiment, Nevada (BREN) tower flights (ref. 8) and the 1987 Boomfile flights (ref. 9). While the findings from each test are significant, neither took concentrated lateral measurements across the transition region. The BREN tower tests focused on vertical measurements, while the Boomfile test had measurements spaced on the order of a mile apart. Both will be discussed in more detail below.

Project Objectives

One of the project objectives for FaINT was to provide a dataset for validation of future shadow side computer models, and for use in empirical analysis. Existing models like the Lossy Nonlinear Tricomi Equation (LNTE) (ref. 10) developed by Pennsylvania State University are not practical to use for full sonic boom carpets, since they take extensive computing core hours to model single sonic boom rays, and have yet to be validated with lateral cutoff data. The FaINT will provide a working reference database as more advanced models are developed. Another objective was to determine or develop an appropriate noise metric to characterize the unique waveforms of sonic booms near the lateral edge of the carpet. Metrics commonly accepted by the sonic boom community, such as Stevens' Mark VII (ref. 11) Perceived Level (PL_{70}) and A-weighted Sound Exposure Level (ASEL) will be found in this paper to be less applicable for the waveform shape of the evanescent waves in the transition and shadow zones. To address this, FaINT intended to develop a quantifiable definition of the audible extent of the sonic boom noise, beyond the bounds of the primary acoustic carpet. Because there is still notable noise beyond lateral cutoff, it is necessary to define an "acoustic lateral cutoff," which encompasses the sonic boom's true envelope on the ground. Another project objective was to analyze the effects of the lower atmosphere on sonic boom rays near the lateral edge of the sonic boom carpet.

Flight Objectives

The success of the test relied heavily on the ability to produce target sonic boom levels and place the edge of the sonic boom carpet accurately and precisely at a specific location on a microphone array on the ground. One of the FaINT flight objectives was to produce these sonic booms using airplane flight assets that were already available to NASA. Achieving this flight objective required an F-18 airplane (McDonnell Douglas, now The Boeing Company, Chicago, Illinois) to conduct straight and level flight profiles at speeds ranging from Mach 1.20 to 1.30 and at altitudes of 35,000 ft to 40,000 ft pressure altitude (Hp). In order to consistently and successfully perform these flight profiles, it was required that, while supersonic, the sonic boom-generating airplane be capable of maintaining a constant heading within 3-deg and Mach number within a ± 0.003 tolerance. This condition would help eliminate off-condition passes, resulting in an aggressive, concise flight phase. It was required that the airplane be capable of performing at least six flight passes in one flight.

Because atmospheric conditions play a significant role in the propagation of sonic booms, upper-atmospheric soundings from a global positioning system (GPS) radiosonde weather balloon were required prior to each flight for mission planning purposes. Upper-atmospheric soundings were also required at takeoff time for post-analysis of sonic boom generation. For similar reasons, it was also a requirement to record meteorological data at ground level.

Test Architecture

Key FaINT test assets consisted of airplanes and instrumentation on the ground. Ground instrumentation was required to measure sonic boom signatures and atmospheric conditions near the ground. The test included two sets of airplanes: one to produce sonic booms, and the other to record sonic booms in the midfield. Other test elements included flight operations and mission planning efforts.

Ground Instrumentation

The array of ground sensors for FaINT consisted of a linear microphone array, a spiral microphone array, and three weather towers (fig. 5) all located on the southwest portion of Rogers Dry Lakebed at Edwards Air Force Base, California. There was also a tethered blimp with microphones attached, provided and operated by Cessna, to record measurements more than 2000 ft above the ground. The blimp and its data is not discussed here, however, because it is beyond the scope of this paper.

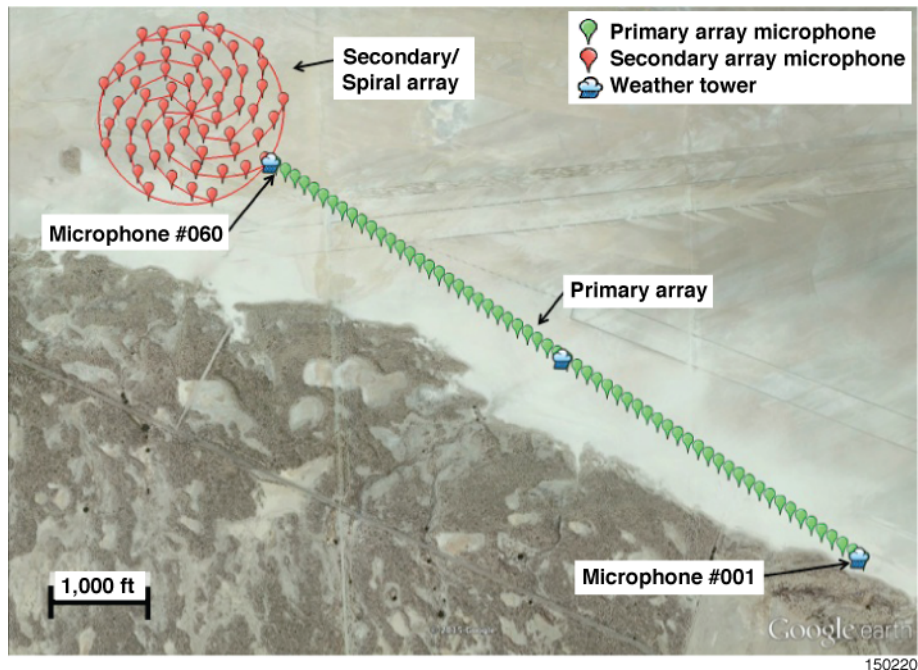


Figure 5. FaINT lateral cutoff round microphone arrays.

Rogers Dry Lakebed offered a very hard and obstruction free area, whose altitude varied less than one foot over the linear arrays, and the spiral array microphones were within 1/16 in of a flat plane, tilted about one arc minute from level, east side down. The orientations of the arrays were selected based on topography of the lakebed shoreline and the available airspace, most notably the High Altitude Supersonic Corridor.

Ground Microphone Arrays

The primary microphone array was linear and consisted of 60 microphones spaced 125 ft apart along a heading of 124-304 deg from true north in order to be perpendicular to the airplane flight path. The individual microphones were labeled #001 through #060, where #001 was on the east side of the array and #060 was on the west side of the array. A spacing of 125 ft was chosen

as a trade-off between desiring little variation from one microphone to the next, due to airplane flight and atmospheric variability, as well as desiring as large an array in distance as possible. There were also constraints with the total number of microphones and recording channels available, as well as limitations with quantity of cables needed and the workforce to deploy, operate, and retrieve the cables and equipment. In all, almost 3 mi of seven-conductor microphone cable and over 8 mi of coaxial Bayonet Neill-Concelman (BNC) cable were used for the linear array. Appropriate cabling was used to ensure that signal attenuation was not a factor considering the extreme distances involved.

On the linear array, Brüel & Kjær (B&K) model 4193 low-frequency microphones (without the UC0211 low-frequency adapter) were used at 47 locations, and GRAS model 40AN low-frequency microphones were used at 13 locations. The two types of microphones are comparable in sonic boom measurement quality. Cables were deployed at the beginning of the program, and remained deployed in the field for the one-week period. Each B&K microphone was covered with a hemispherical foam windscreens, and used a B&K preamplifier model 2669C. Microphones were calibrated pre- and post-flight with a B&K model 4231 sound calibrator set at 94dB. The microphone data was adjusted by being given a calibration gain, which was based on the difference between the measured signal root-mean-squared (RMS) and the theoretical calibrator RMS. Brüel & Kjær model 2690-0S4 Nexus amplifiers were used to raise the maximum signal voltage up to +/- 10VDC. Fifteen Nexus amplifiers were used on groups of four microphones. From the Nexus amplifiers, long BNC cables provided the signals to four analog-to-digital converters and recorders distributed along the array. Three Ling Dynamic Systems (LDS) Dactron brand Focus recorders were used on microphones #001 through #029. A National Instruments model 4472 PXI recorder was used for microphones #030 through #060. Each of the four recorders also recorded GPS-based IRIG-B timecode on one channel for later consolidation of all the datasets.

The spiral microphone array data was gathered to investigate directionality of the sonic boom propagation at lateral cutoff. Phased spiral designs are a heavily utilized method for acoustic beamforming. Beamforming analysis techniques are widely used for identifying the location and imaging of acoustic disturbance sources, such as aircraft engine noise (ref. 12). The center of a 1000-ft radius spiral microphone array provided and operated by the Boeing Company was positioned at the extended line of the linear array. Details of the spiral array are discussed in Appendix A. This paper will focus exclusively on the data collected by the primary linear array. The data from the secondary spiral array will be investigated in the future.

All microphone locations were computed with geodesic software and located using a Javad Triumph-VS carrier-phase differential GPS system to within about an inch. At each microphone location, a 2 ft by 2 ft by 3/4 in sq of plywood was used as a ground board, with the primary microphone centered on the board, and the second microphone, for those seven locations with two microphones, halfway between the center and the edge of the board (fig. 6). A sheet metal template and environmentally safe water-based blue spray paint was used to mark each location on the dry lakebed with an "X" that would define the location for the corners of the ground board.

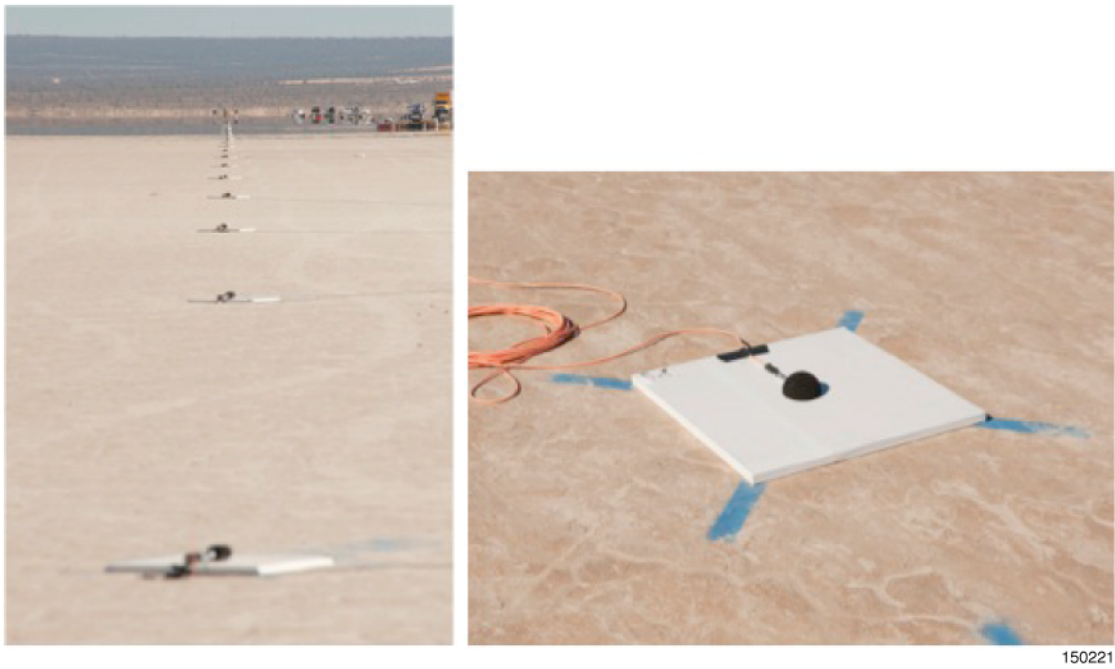


Figure 6. Microphones on ground boards.

Meteorological Systems

For pre-flight mission planning and post-flight sonic boom analysis, atmospheric sounding data were gathered using an airborne weather measurement package consisting of a Lockheed Martin (Bethesda, Maryland) model LMS6 radiosonde unit. The unit was able to measure temperature, relative humidity, pressure, wind direction, and wind speed derived from GPS differential measurement at a ground station and the radiosonde. This package provided data from near-ground up to the flight altitudes of the airplane.

Ground-level meteorological measurements for post-flight sonic boom analysis were taken using solar-powered surface weather towers that measured temperature, humidity, wind direction, wind speed, and pressure at GPS time-synced 0.5 s increments. The pressure, temperature, and wind sensors were at heights of approximately 4 ft, 6 ft, and 10 ft above the ground, respectively. Three weather towers were located 100 ft from microphones #001, #030, and #060, perpendicular to the array line and on the southern side of the arrays.

Aircraft

F-18 Airplane

NASA Armstrong F-18B airplane, tail number 852 was used to generate the sonic booms for FAINT. Tail number 852 is a standard F-18B airplane, and was configured with a centerline fuel tank. Internally, this aircraft is equipped with a Research Quick Data System (RQDS) that converts the airplane's 1553 bus data into pulse-code modulation data for telemetry and onboard recording. GPS-based IRIG-B timecode generator data were also recorded.

Accurate placement of the sonic boom footprint on the microphone array required accurate knowledge of the Mach number and altitude of the airplane. The calibration of the airplane production air data system in the supersonic region has known errors on the order of 0.045 Mach number, which can result in up to a 1.7 nm error in sonic boom location (ref. 13). For the range of

Mach numbers flown during FaINT, this error has been shown to be approximately +0.02 Mach number (ref. 14), and has been corrected appropriately in the data presented here.

Airborne Acoustic Measurement Platform (AAMP)

The TG-14 motorglider, tail number 149, shown in figure 7, was used to measure the sonic booms for FaINT above ground-level turbulence. The TG-14 airplane was a NASA-operated US Air Force Test Pilot School airplane, and is equipped with an acoustic sensor to make up the Airborne Acoustic Measurement Platform (AAMP). Figure 7 shows the wingtip mounted B&K model 4193 0.5-inch condenser microphone with a B&K model UC0211 low-frequency adapter, B&K model UA0386 tapered nose cone, and B&K model 2669C preamplifier. This was connected to the instrumentation pallet in the cargo area shown in figure 8. The microphone was amplified by a B&K model 2690-A-OS2 Nexus amplifier, and then digitized by a LDS Dactron Focus II analog to digital converter. Cockpit audio was also digitized by the Focus II. LDS Dactron RT Pro software hosted on a Fujitsu P1630 tablet PC computer was used to record the data. Instrumentation Technology Systems model 6155D GPS-based IRIG-B timecode generator data was also recorded. An Ashtech Z-Xtreme carrier-phase differential GPS receiver measured the position and velocity of the TG-14 airplane. All these systems were battery powered.



Figure 7. Wingtip mounted microphone on TG-14 tail number 149, with inset closeup of microphone.

It was discovered during checkout-flights that the microphone portion of the AAMP system would not record properly when the propeller of the airplane was rotating. To address this, prior to recording sonic booms the airplane engine was turned off and the data was collected during gliding flight. The engine would be restarted to position the airplane for the next supersonic pass of the F-18 airplane. Positioning of the TG-14 airplane was aided by a Garmin model GPSMAP 496 handheld GPS receiver.

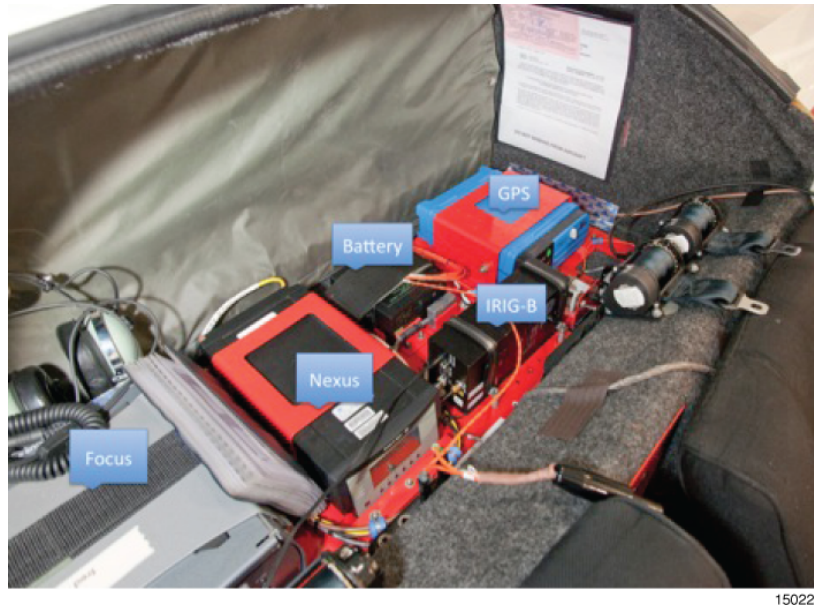


Figure 8. TG-14 instrumentation pallet. From left to right: Focus recorder, Nexus amplifier, battery, GPS-base IRIG-B timecode generator, Z-Xtreme GPS receiver.

Flight Operations and Mission Planning

The basic test setup used for the lateral cutoff experiment is illustrated in figure 9. To capture the lateral cutoff region of the sonic boom carpet, an F-18 aircraft was flown supersonically straight and level for a period of time so as to generate a consistent shock that would intersect the ground microphone array. The isopemps in figure 9 represent the location where the shock ray cone, generated at a given time, intercepts the ground. It was attempted to place the lateral cutoff region, illustrated by the red line near microphone location #020, along the ground array so as to capture the full N-wave shock along with the zone where the shock refraction occurs, and also the region after full refraction.

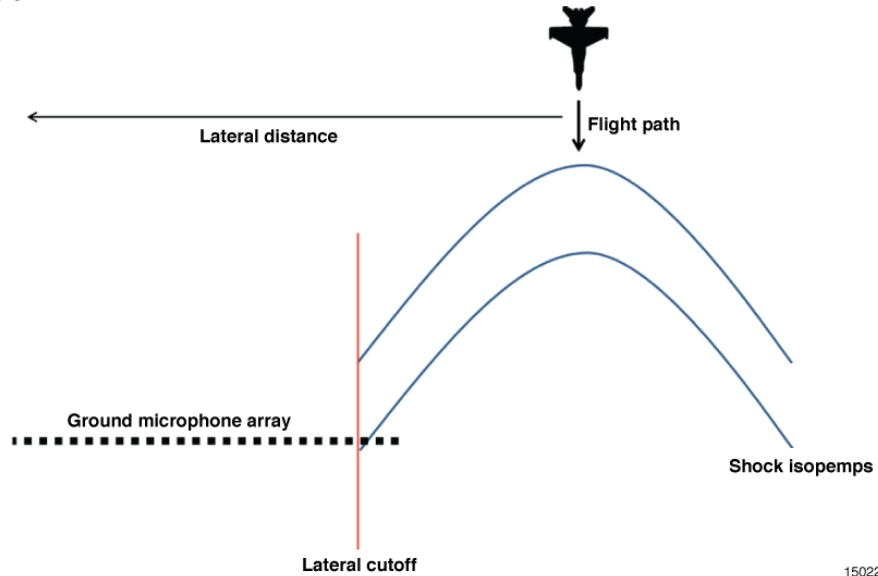


Figure 9. Basic test setup for FaINT lateral cutoff tests, depicting a subset of deployed instrumentation (not to scale).

For FaINT mission planning, a preflight GPS radiosonde weather balloon was launched to gather the atmospheric sounding. A trajectory of a theoretical straight and level flight pass was used as a template maneuver, and adjustments were made considering the day-of-flight atmospheric conditions. These data were then run through PCBoom (ref. 14), a sonic boom propagation prediction computer package developed by Wyle, to give a theoretical sonic boom footprint. The F-18 airplane waypoint was translated to place the lateral edge of the sonic boom at microphone #020. The F-18 airplane was to be flown steadily at the intended heading (perpendicular to the microphone array), altitude, and Mach number, from 15 seconds before to 15 seconds after reaching the waypoint. The planned overpressures for a particular flight pass were a function of the required flight heading, altitude, and Mach number to place the lateral edge of the sonic boom at microphone #020, given the atmospheric conditions.

During flight, in-the-field ground personnel used audible cues to adjust the F-18 airplane waypoint as necessary. After each pass, ground personnel along the microphone array would subjectively report the type of sonic boom sound heard using predefined visual signals. Based on this feedback, the F-18 airplane pilot could, if necessary, be instructed by way of radio communication link to shift the trajectory parallel either east or west, shifting the sonic boom carpet appropriately. For example, a distinct in-carpet N-wave heard at microphone #040 would require a parallel shift east.

For each flight, the TG-14 airplane AAMP had planned to be flown at approximately 4500 ft above the ground. The intent was to collect sonic boom measurements above most of the atmospheric turbulence near the ground. The same PCBoom sonic boom propagation code was used to predict the location of the sonic boom ray that would intersect the microphone array at location #020, 4500 ft above the ground. The intent was to record the same propagation ray at both 4500 ft above ground, and on the ground. PCBoom provided a predicted time, latitude, and longitude. The AAMP was flown to intersect the sonic boom ray at that time and location.

Test Point Matrix

Lateral cutoff tests for FaINT consisted of seven flights over four days. Each flight used an F-18 airplane as the sonic boom source. There were 37 lateral cutoff flight passes total, ranging from 35,300 – 40,600 ft Hp and Mach 1.223 – 1.286. Table 1 lists the mean flight conditions as flown by the F-18 airplane during each pass. It should be noted that these are average values. The actual conditions at the exact time the F-18 airplane produced the recorded sonic booms are unknown because the computer tools required to correlate which flight condition corresponds with which measurement on the ground near the sonic boom carpet edge do not exist at this time.

Table 1. FaINT F-18 airplane lateral cutoff test point matrix.

Date	Flight Number	Pass Number	Mach	Altitude (ft Hp)	Heading (degrees, true)	Steady ?
October 29, 2012	1	1	1.226	35510	215	Y
		2	1.230	35580	216	N
		3	1.234	35500	216	N
		4	1.229	35500	216	N
		5	1.225	35430	217	N
	2	1	1.248	40230	218	Y
		2	1.257	40450	218	Y
		3	1.243	40170	217	Y
		4	1.261	40580	218	Y
		5	1.261	40500	217	Y
October 30, 2012	3	1	1.286	37510	217	Y
		2	1.281	37810	218	Y
		3	1.277	37960	220	N
		4	1.276	38000	219	N
		5	1.279	37670	219	N
		6	1.279	37450	218	Y
	4	1	1.227	35690	217	N
		2	1.229	35400	216	Y
		3	1.231	35800	218	N
		4	1.238	35840	217	Y
		5	1.228	35490	216	N
		6	1.237	35460	217	N
October 31, 2012	5	1	1.230	35380	215	N
		2	1.223	35310	215	N
		3	1.230	35420	214	N
		4	1.227	35480	215	Y
		5	1.234	35530	217	Y
	6	1	1.228	37520	217	Y
		2	1.235	37400	215	Y
		3	1.237	37580	216	Y
		4	1.237	37400	215	Y
		5	1.224	37640	216	Y
November 1, 2012	7	1	1.263	35360	216	N
		2	1.264	35490	216	Y
		3	1.266	35470	216	N
		4	1.261	35500	216	Y
		5	1.263	35460	214	N

Analysis was performed to establish a yes/no criterion, describing whether the F-18B airplane was steady during the flight pass. The standard deviations for Mach, altitude, and heading were computed for each flight pass. The average value of the standard deviations of each parameter across every flight was used as a threshold to determine steadiness. For a given flight pass, if two or more of the three flight parameters had standard deviations above the threshold, the pass was deemed to be unsteady.

Analysis and Results

Research emphases of this paper will focus on an appropriate metric for describing sonic boom waveforms at the sonic boom carpet edge; a quantifiable definition of the lateral extent of a sonic boom's noise region; overpressure profiles as a function of lateral distance from the flight path; and airborne, midfield measurements of sonic booms near the carpet edge. While FaINT involved the use of a spiral microphone array to study directionality of sonic booms, this paper will not include that research.

Appropriate Metrics for Lateral Cutoff Acoustics

Overpressure alone is not sufficient for all sonic boom analysis, because peak values do not offer insight into characteristics such as frequency content, rise time, and signature length. Capturing these characteristics is essential to understanding sonic booms in the transition region and shadow zone. Metrics used by the sonic boom community, such as the 70ms integrated (ref. 7) Stevens' Mark VII (ref. 11) PL (PL_{70}), may be less applicable for the waveform shape of the evanescent waves in the transition and shadow zones. The acoustic signature in these regions is highly variable in duration and impulsiveness, and the short integration time of the PL_{70} metric is not well-suited for these longer, duration-varying sounds.

As is evident in figure 4, for high intensity, impulsive N-signatures, finding the start and end times is fairly straight forward, as there is a very high signal to noise ratio. As the signature decays, finding the start and end points becomes more difficult, since the pressures caused by the shock become less stark in comparison to the ambient noise and post-boom noise. The start and end times of each signature was found through energy analysis. Total energy of the signal was found by integrating the square of the pressures. The point in the signature where 99 percent of the total signal energy had been expended was declared the end point, and the remainder of the signature was discarded. The total energy of the new signature was then found, and stepping backwards through the new signature, the start point was found at the point 99 percent of the energy from the end point had been expended. Since noise becomes a greater percentage of the energy as the signatures decay, the duration was capped at 2 s to avoid including excessive after-boom noise for the quieter signatures. The 99-percent value was chosen by trial and error, and resulted in the most consistent and accurate windowing of the raw signatures. The pressure signatures in figure 4 illustrate the results of the windowing procedure.

An alternate acoustic metric may be more applicable for signatures of the type experienced in the lateral cutoff region. This metric uses Stevens' PL as a method of frequency weighting, with the input determined by Sound Exposure Level (SEL) 1 s normalized method of integration defined in ISO 1996 (ref. 15). This metric is referred to as Perceived Sound Exposure Level (PL_{SEL}). The 1-s normalized method of energy integration used for PL_{SEL} is more applicable to the longer 500 ms to 2 s duration signatures seen in the region beyond lateral cutoff. The traditional 70 ms integrated PL_{70} metric used within the boom carpet will grow disproportionately quickly as the signature increases beyond 300 ms in length, and therefore is not applicable to the longer rumbles experienced outside of the carpet.

Figure 10 shows a comparison between PL_{SEL} and other commonly used sonic boom acoustic metrics for several FaINT flight passes. Other metrics shown are fast A-weighted exponential-

time-averaged sound pressure level (LAF), slow A-weighted exponential-time-averaged sound pressure level (LAS), ASEL, and C-weighted Sound Exposure Level (CSEL). These metrics were calculated using standard procedures described in ISO 1996 (ref. 15) and ANSI S1.4 (ref. 16).

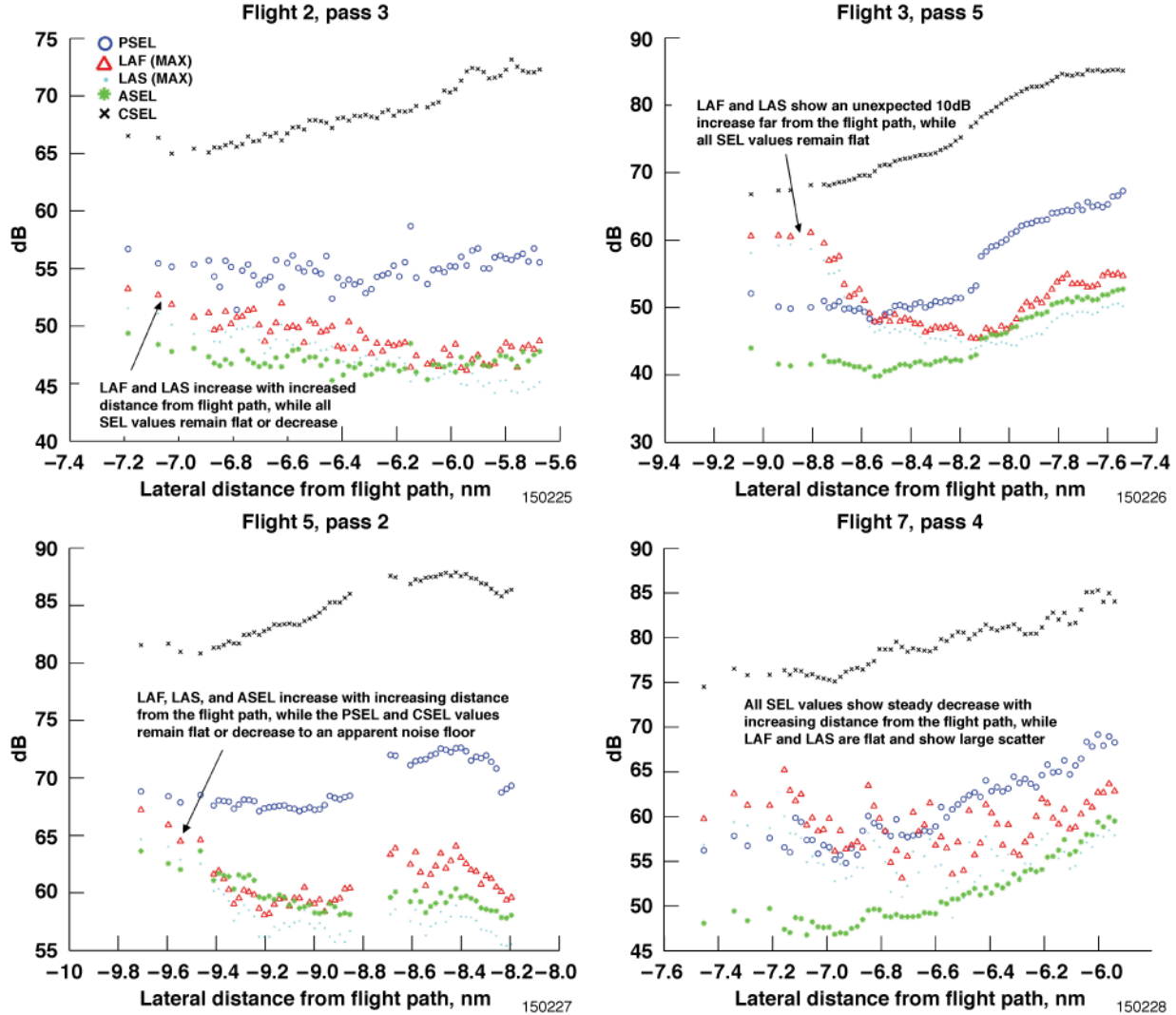


Figure 10. Acoustic levels near the transition region as a function of lateral distance for passes showing a discrepancy between SEL and continuous metrics.¹⁵

As shown, most of the PL_{SEL} and CSEL values aligned with the expected acoustic profile beyond lateral cutoff better than the other metrics. The PL_{SEL} and CSEL metrics are seen hitting a noise floor where the acoustic energy of the sonic boom has completely dissipated, and only the ambient noise is remaining. The continuous exponentially weighted metrics, (LAF and LAS) are much more susceptible to after-boom ambient noise, and the A-weighted metric is more sensitive to higher frequency, non-boom related noise. Because of the better performance of the SEL method of energy integration for comparing the sounds of varying durations, along with Stevens' PL being an industry-accepted frequency weighting for sonic boom measurements when compared with C-weighting, PL_{SEL} was used to analyze sonic booms near lateral cutoff in this paper.

Acoustic Lateral Cutoff Definition

With ray tracing programs, such as PCBoom (ref. 1), computed lateral cutoff occurs when the computed ray path is tangent to the ground (fig. 3). These computations are only as accurate as the airplane Mach number, altitude, ground elevation, temperature, and wind vertical profile used as input to the program. For long propagation distances, a spherical or oblate spheroid earth model is used instead of a locally flat earth representation. Small increments in phi angle are used near the carpet edge to more accurately define the computed lateral cutoff; this switches to $\Delta\phi$ angle of 0.01 degrees near the edge.

This paper will attempt to determine a qualitative definition for the acoustical lateral cutoff. In order to do so, it is useful to discuss the history of lateral cutoff investigation. There are two previous studies prior to FaINT that involved lateral cutoff measurements; the BREN tower flights and the Boomfile flights. These will now be briefly discussed with salient features and limitations as compared to the FaINT effort, starting with the Bare Reactor Experiment, Nevada (BREN) tower flights in 1970 (ref. 8). With the ground-level data alone, it was quite difficult to determine the lateral cutoff location, but the researchers found that the elevated microphones on the tower allowed the computation of the shock wave inclination angle. A value near zero indicated the ray path was tangent to the ground, which is lateral cutoff. Their analysis of computed lateral cutoff agreed with the measured data within about ± 1.0 km (± 3300 ft). These measurements were on the leeward (downwind) side of the carpet with a strong crosswind.

In the current FaINT dataset, as well as the 1987 Boomfile flights (ref. 9), both digital recordings and “ear” witness reports of N-wave shocks and/or rumbles that occur beyond the computed lateral cutoff have occurred, with 70 such events noted in the Boomfile report. The Boomfile dataset analysis suffers from several limitations. The biggest deficiency lies in the use of the 1972 Standard Atmosphere instead of the measured rawinsonde balloon data for computing the lateral cutoff. The flights were flown in the hot desert July/August timeframe, with weather conditions far from the 1972 Standard Day temperature profile. The flights were flown toward the west, against the prevailing winds of the region, which would tend to shrink the lateral carpet width. Other deficiencies are a lack of steady-state flight conditions, as shown in the Boomfile dataset by the presence of multiple shock patterns including U-waves, and an unknown pedigree of the many aircraft type airdata calibrations. It is noted that the production F-18 airplane airdata system has Mach number errors up to 0.045 in the supersonic regime (ref. 13). The Boom Event Analyzer Recorder (BEAR) sensors used during Boomfile may not have autonomously triggered for some of the quieter rumble, or may have been artificially triggered by nearby truck noise. The Boomfile dataset does have some of the widest available recordings for lateral cutoff; up to 24 statute miles in length, but individual ground measurements were on the order of a mile apart. Perhaps this dataset can be revisited with more modern propagation code versions and use the actual measured weather data to more accurately determine the computed lateral cutoff. The FaINT dataset, while not nearly as wide, should not suffer from the above listed analysis deficiencies, but still recorded significant events beyond computed lateral cutoff. The FaINT data were all taken on the windward side of the carpet. In retrospect, some data should have been taken on the leeward side as well.

In summary, two earlier lateral cutoff efforts were conducted before FaINT. First, the BREN tower flights included the use of elevated microphones above the ground microphones to directly measure when propagation was tangent to the Earth's surface (the definition of lateral cutoff), and data were collected on the leeward side of the carpet. The FaINT array did not use elevated microphones (beyond the motor glider and blimp), as it was deemed more important to make as long of an array as possible. Taking some additional FaINT data on the leeward side of the carpet was overlooked. Second, the Boomfile flights had an extremely wide array, but suffered from issues with improperly applied atmospheric data, unknown air data accuracies, unsteady test

points, and instrumentation issues of that era. The FaINT effort did not suffer from these issues of the Boomfile dataset.

The concept of “acoustical lateral cutoff” is now defined as the location to the side of the airplane track where the noise is no longer distinguishable relative to ambient noise. It may be quantified by a future regulatory sonic boom noise limit, such as “X” decibels, or by a certain maximum overpressure value along with a minimum rise time. Audible and measureable effects of supersonic flight were heard beyond the computed lateral cutoff, but these may or may not be significant, depending on the level of noise limit selected.

To determine a quantitative acoustic lateral cutoff based on FaINT data, first an acoustic noise floor was determined. Approximately half of the test points showed PL_{SEL} approaching an apparent asymptote with increasing lateral distance. The sound level at which the microphones appeared to no longer discern a sonic boom signal was considered the ambient PL_{SEL} floor. Figure 11 shows the test point with the lowest recorded overpressures. Measurements start nearly 2 nm beyond the lateral cutoff predicted by PCBoom. While the overpressures (ΔP) continue to decrease with increasing lateral distance, PL_{SEL} has clearly reached the ambient noise floor. Test points similar to this were used to calculate a noise floor of 58.6 dB PL_{SEL} .

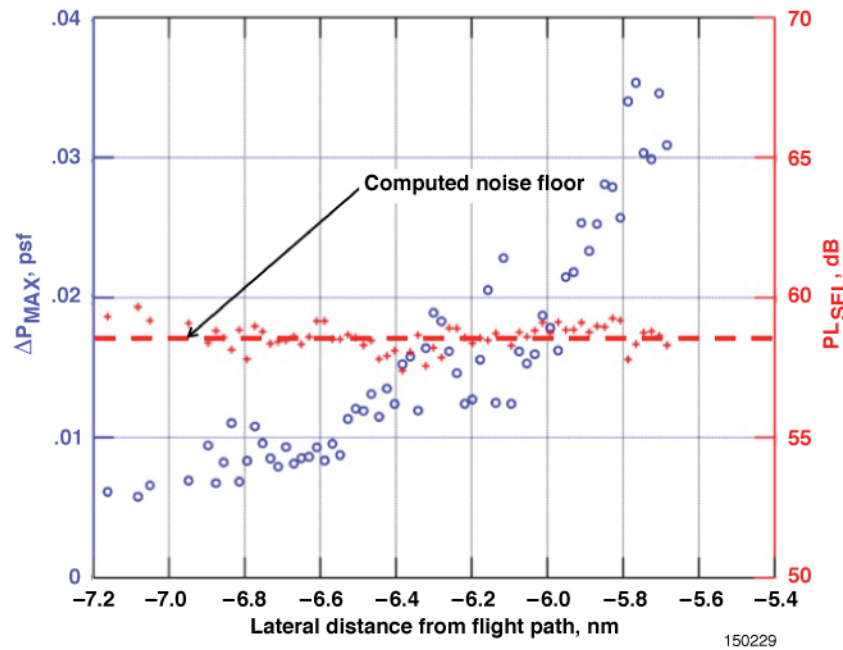


Figure 11. Computed noise floor from sonic boom measurements compared to flight 2, pass 3.

After looking at each FaINT test point, it is apparent that at four times the acoustic power (or +6 dB) of the ambient noise, lateral sonic boom profile characteristics are consistently discernable. This observation led to the postulation that 65 dB PL_{SEL} is a reasonable threshold for defining acoustic lateral cutoff.

Overpressure/Metrics versus Lateral Distance

Real data knowledge of the sonic boom propagation at the lateral cutoff will give researchers an understanding of noise levels beyond where current, common sonic boom prediction tools are able to model. Considerable sound levels can be experienced far beyond the predicted sonic boom carpet due to the difficulties in accurately modeling both the evolution of N-waves within the sonic boom carpet, and evanescent waves that propagate in the shadow zone. Sonic boom levels are generally expected to reach a pressure peak toward the middle of the sonic boom

carpet, and decay with increased proximity to the carpet edge, similar to a bell curve (fig. 1). Airplanes with outer mold lines designed and shaped to produce “low sonic booms” (sonic booms intended to be comparable to future commercial supersonic airplanes), however, may produce unorthodox sonic boom carpets, with the peak levels several miles away from the airplane’s flight path. If this is the case, knowledge of sonic boom propagation near the carpet edge is essential.

A majority of ground measurements taken during Faint demonstrated the expected profile of sonic boom magnitude with increasing distance from the airplane’s flight path beyond lateral cutoff. Evanescent waves are acoustic waves with an intensity that exhibits exponential decay. Figures 12 and 13 illustrate two select examples. Both measurements are beyond the lateral cutoff predicted by PCBoom. Each figure shows a steady, exponential-like decrease of both overpressure and PL_{SEL} . Note that both figures show an errant data point at microphone #020 (at approximately 0.45 nm from microphone #001), which is considered to be due to a faulty measurement.

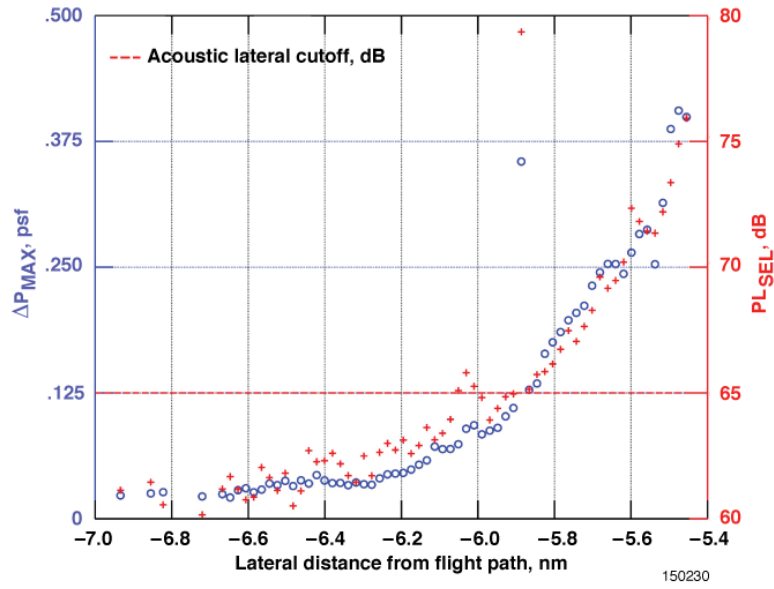


Figure 12. Lateral ground measurements. Flight 2, pass 4.

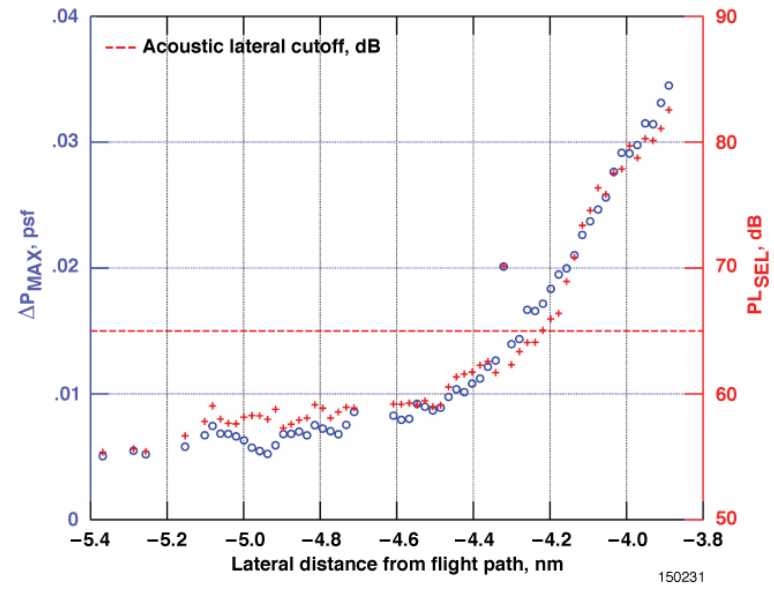


Figure 13. Lateral ground measurements. Flight 4, pass 5.

Several important observations are derived from these plots. First, the acoustic floor can be inferred as approximately -6.6 nm for flight 2 pass 4, and -4.7 nm for flight 4 pass 5, when PL_{SEL} reaches the asymptote of ambient noise at about 60 dB. Second, the data shows that the mission planning techniques are capable of accurately capturing the carpet edge. Third, the data supports the previously suggested 65 dB PL_{SEL} as a reasonable threshold for defining acoustic lateral cutoff. Using this criterion, 18 of the 37 FaINT test points resulted in the successful placement of the acoustic lateral cutoff on the microphone array (appendix B).

The difference in sonic boom carpet width between flight 2 pass 4 and flight 4 pass 5 is most likely due to the airplane flight conditions. Wind directions were comparable for each pass, generally coming from the west-southwest direction. The largest attribute to the wider carpet of flight 2 pass 4 was that it was flown 5000 ft higher (table 1).

The well-behaved nature of the profiles in figures 12 and 13 are likely due to the lack of strong temperature inversion near the ground. Several other possible influences were investigated, including atmospheric turbulence, steadiness of flight, and wind speed and direction at ground level. Flight 2 pass 4 was steady; with low-altitude winds under 5 knots, and practically no turbulence. Conversely, flight 4 pass 5 was unsteady, with low-altitude winds maxing out at 9 knots and light turbulence. The weakness of the temperature inversion near the ground, as shown in figure 14, was shown to correlate strongly with a smooth lateral carpet transition. Both flights 2 and 4 occurred in the late morning, as the ground began to warm and the temperature inversion from the early morning began to disperse. Conversely, figure 15 shows a strong temperature inversion during the early mornings when flights 1 and 5 took place.

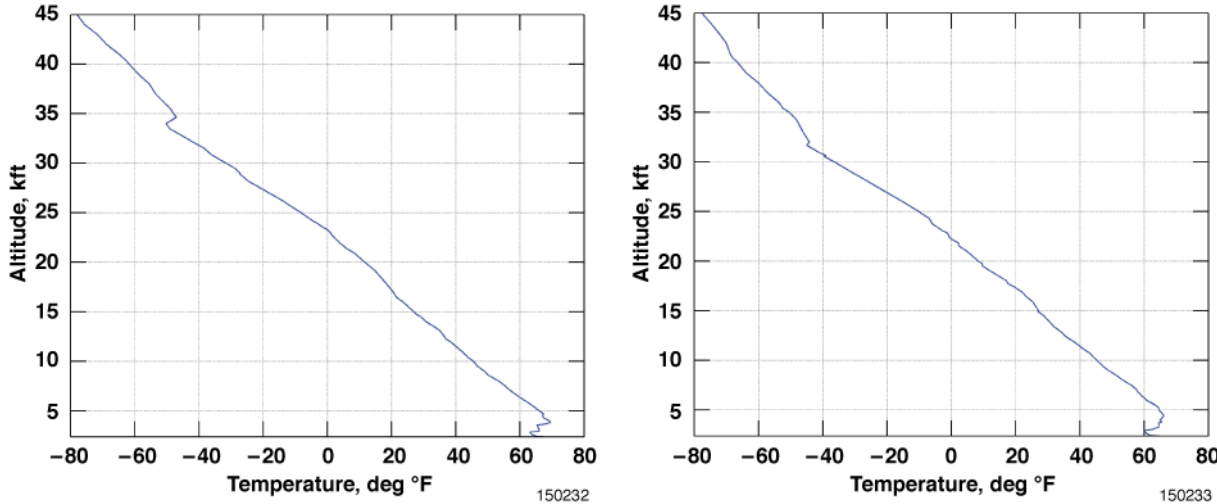


Figure 14. Atmospheric temperature profile during flight 2 (left) and flight 4 (right), showing a weak temperature inversion.

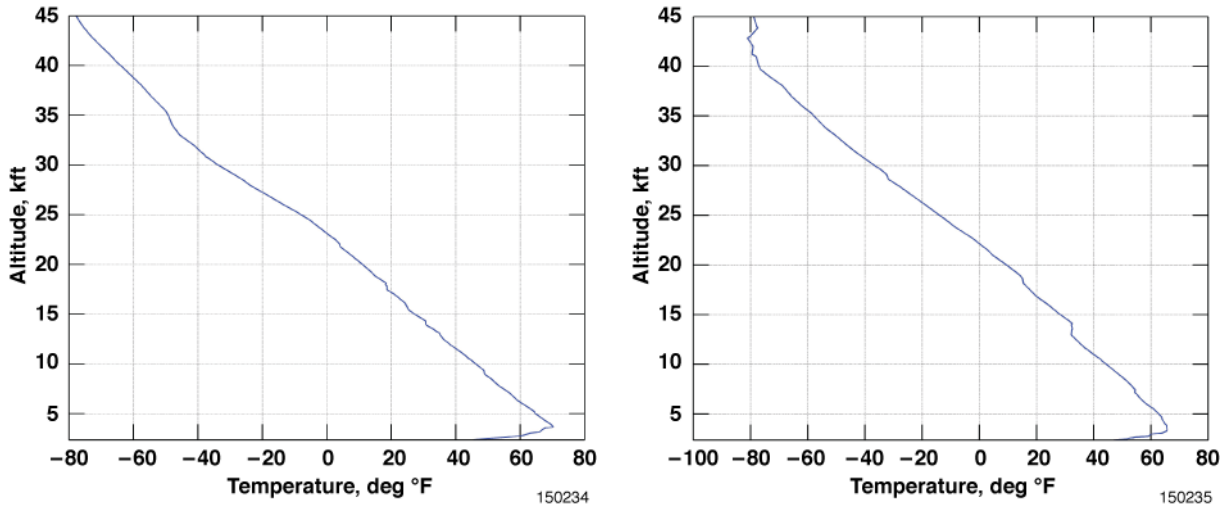


Figure 15. Atmospheric temperature profile during flight 1 (left) and flight 5 (right), showing a strong temperature inversion.

The presence and strength of a temperature inversion on the ground has a considerable influence on the lateral profile of a sonic boom carpet near the edge. Figures 16 and 17 show strong oscillations in PL_{SEL} , in stark contrast to the previous examples. Both of these measurements are also beyond the lateral cutoff predicted by PCBoom.

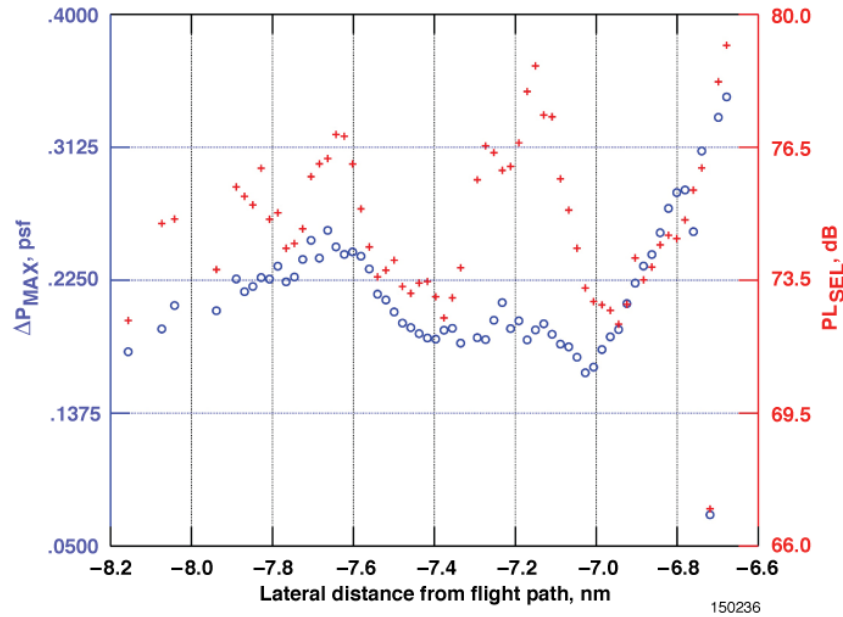


Figure 16. Lateral ground measurements. Flight 1, pass 1.

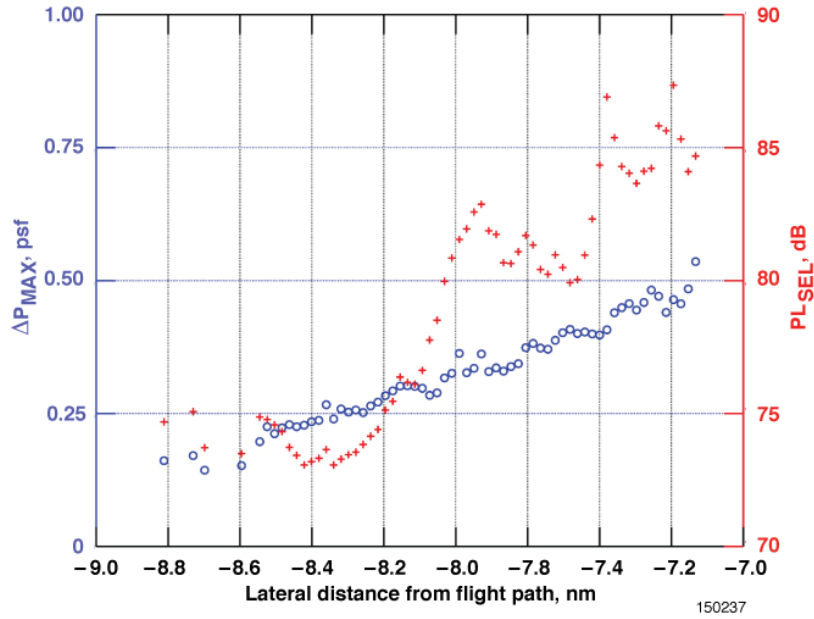


Figure 17. Lateral ground measurements. Flight 5, pass 1.

An observer could infer that the lateral measurements shown for flight 1 pass 1 (fig. 16) are expected to quickly and exponentially decrease in magnitude from the highest level at -6.7 nm, to a lowest at -8.2 nm, under ideal conditions. The temperature inversion, however, contributes to a PL_{SEL} of more than 76.5 dB, nearly a nautical mile further laterally from the location of the highest measured magnitude. This can be compared to a PL_{SEL} below 60 dB at the same lateral distance for flight 4 pass 5 (fig. 13). Considering that the flight conditions for each flight pass are not substantially different –a difference of only -0.004 Mach and +20 ft Hp, as shown in table 1– it can be concluded that a strong temperature inversion can cause significant oscillations in PL_{SEL} , greatly increasing the acoustic lateral cutoff. Such high PL_{SEL} at so great a lateral distance is not common for flights during weak temperature inversions.

Midfield Lateral Measurements

The TG-14 airplane AAMP flew at approximately 4500 ft above the ground in an effort to collect sonic boom measurements above most of the atmospheric turbulence near the ground. It was flown such that it would attempt to measure the sonic boom ray that would intersect the microphone array at location #020. The intent was to record the same sonic boom ray at both 4500 ft above ground, and on the ground. PCBoom provided a predicted time, latitude, and longitude. Then the AAMP was flown to intersect the sonic boom ray at that time and place.

It is not possible to know for certain whether or not the AAMP successfully recorded the exact same sonic boom ray that was recorded on the ground microphone array, since only computer models can do sonic boom ray tracing and are not reliable at lateral cutoff. PCBoom could not provide solutions for 31 out of 37 FaINT flight passes, because it is designed to only model ray propagation, which does not include the transition or shadow region (fig. 3). The FaINT intended to record the acoustic edge, while PCBoom only computes to the extent of the sonic boom limiting ray. This section attempts to empirically show the capability to successfully record the “same” sonic booms 4500 ft above ground, as on the ground at the carpet edge. By using the AAMP to record the shadow side of the sonic boom carpet, the investigation of the same characteristics on the ground discussed in section IV.C can be extended to 4500 ft above ground.

As previously shown, the typical profile for sonic boom overpressure at the edge of a sonic boom carpet for an N-wave generating airplane is an exponential decay in magnitude. Such was the case with most of the FaINT test-points. The typical profile is again illustrated in figures 18 and 19. The figures show the freefield pressure measurements of both the ground microphones and the AAMP microphone on the left vertical axis. The freefield pressure on the ground is the ground microphone measurements with the effects due to ground reflection removed. The ground measurements were divided by a reflection coefficient of 1.27, chosen based on previous estimates of ground reflection coefficients of evanescent waves (ref. 8). The right vertical axis shows the altitude of the F-18 and AAMP in feet above mean sea level (MSL). The altitude is an attempt to show the lateral curvature of the sonic boom propagation, which emphasizes the difficulty in correctly capturing the lateral edge profile.

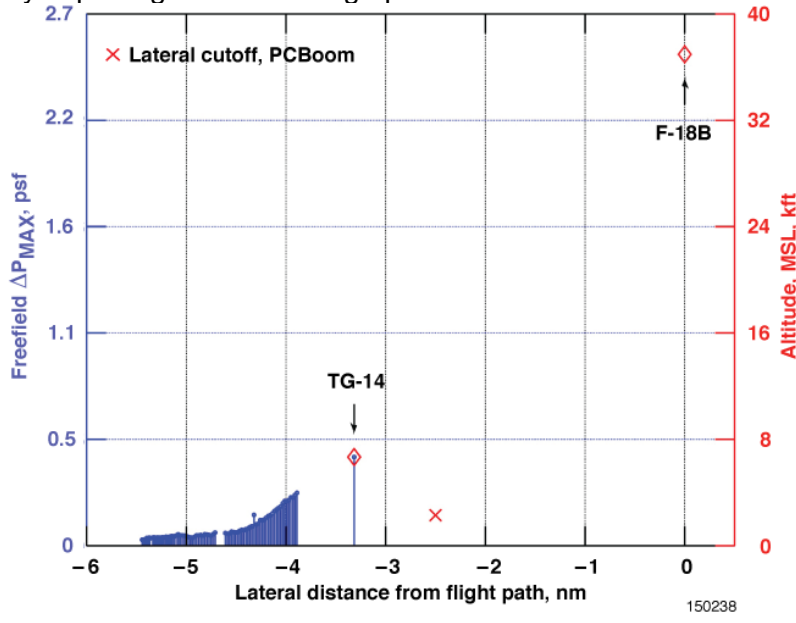


Figure 18. Midfield lateral measurements. Flight 4, pass 5.

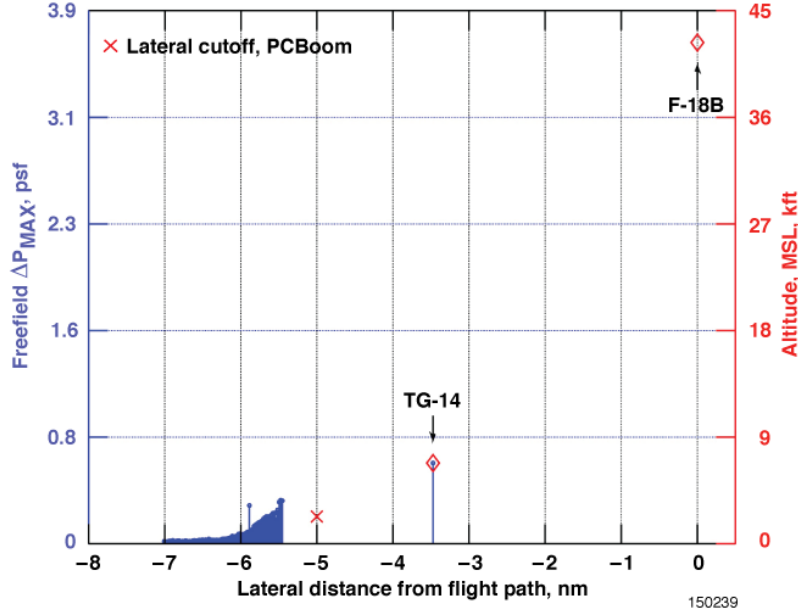


Figure 19. Midfield lateral measurements. Flight 2, pass 4.

Just like earlier examples (figs. 12 and 13), the microphones show a well-behaved decay at the carpet edge, further supported by the AAMP measurements seemingly aligning with the profile. Additional midfield lateral measurements can be found in appendix C.

Some AAMP measurements provided unique results. Figure 20 shows an unexpected lateral sonic boom profile. For this flight pass, most of the microphone array was predicted to be within the primary sonic boom carpet. It is not apparent what test characteristics might have caused such a result, however it should be noted that this is the narrowest carpet measured. It reaches 65 dB PL_{SEL} at -3.2 nm (appendix B), most likely due to having one of the slowest average Mach numbers (1.227). The Mach number could possibly be even lower at the time the sonic boom was generated. Previous examples showed that, other than the strength of a temperature inversion and airplane steadiness, no test conditions that were investigated had notable effects on the lateral sonic boom profile near the carpet edge. Given this assertion, one possible interpretation of flight 4 pass 1 is that the lateral sonic boom profile for the F-18 airplane is not the expected shape at the FAINT flight conditions (fig. 1). A similar conclusion could be drawn from the Boomfile dataset (ref. 9).

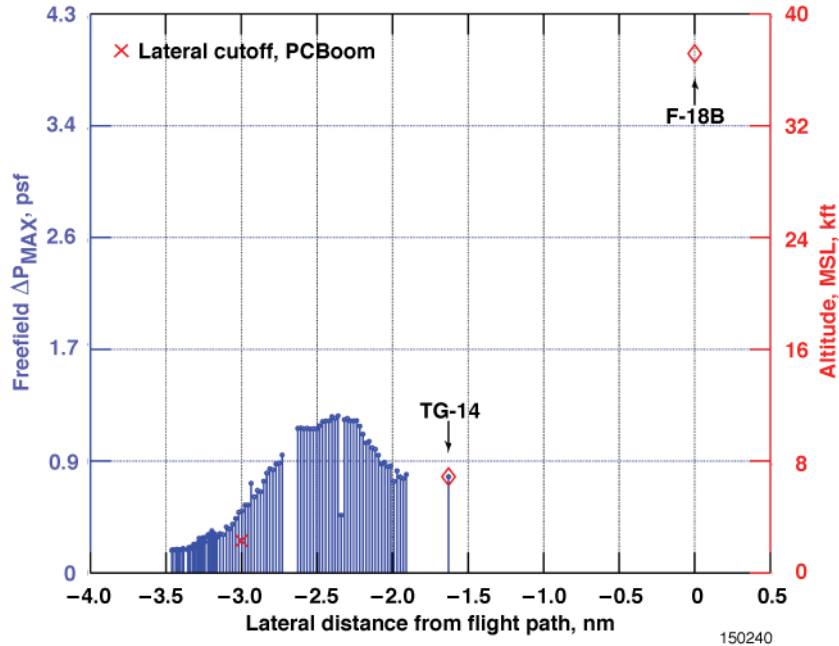


Figure 20. Midfield lateral measurements. Flight 4, pass 1.

Computer Model Comparison

The major assumption of this study hinged upon the notion that modern sonic boom propagation computer models are more accurate toward the center of the sonic boom carpet, less accurate in the transition region, and provide no solution in the shadow zone. To address this assertion, analysis was done by way of comparing PL_{SEL} from predictions (from PCBoom Burgers (ref. 14) solver) using real airplane and atmospheric data as inputs, to actual sonic boom measurements. “Real” data is defined as real-time airplane time-speed-position information, corresponding atmospheric sounding data, and corresponding sonic boom ground measurements.

The FAINT effort produced 37 lateral cutoff flight passes, and PCBoom predicted that the primary sonic boom carpet was on the microphone array for five of those passes. This is because while PCBoom was used as an initial mission planning tool, adjustments were made based on

what was heard on the ground to place the transition and shadow zones on the microphone array. PCBoom predicted a sonic boom on the microphone array for: flight 2 pass 1, flight 3 pass 1, flight 3 pass 2, flight 4 pass 1, and flight 4 pass 6. A sonic boom on the microphone array was also predicted for flight 3 pass 3, however, this flight pass was disregarded due to out-of-tolerance flight conditions.

It was still assumed that the edge of the carpet modeled by PCBoom would be relatively close to the acoustic lateral cutoff. This section investigates the acoustic level and size of the shadow zones by comparing the acoustic lateral cutoff with the primary sonic boom carpet as computed by PCBoom. Figures 21 and 22 are two of the five cases where PCBoom predicted a lateral cutoff (LCO) on the microphone array.

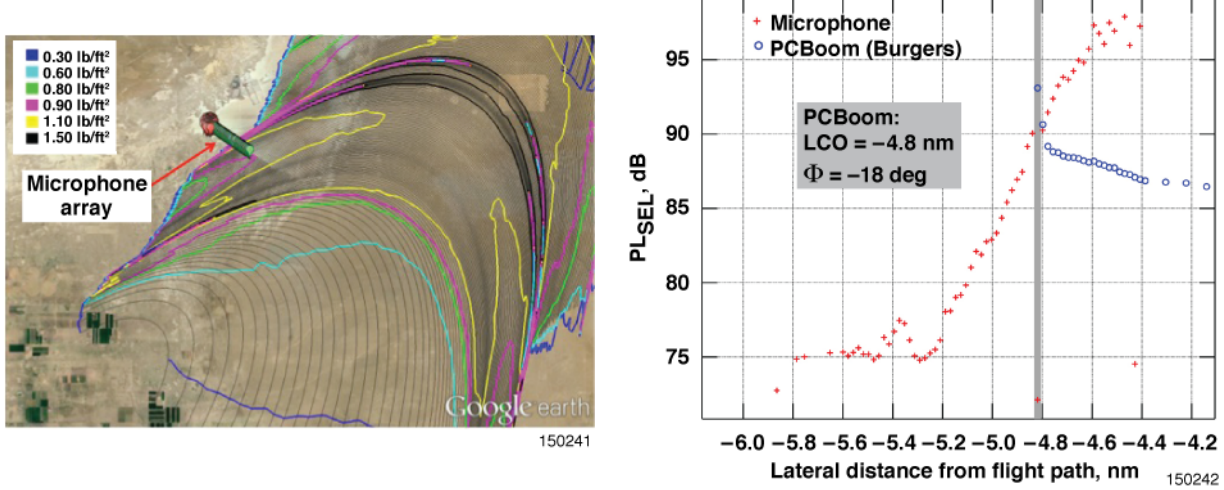


Figure 21. Predicted PCBoom sonic boom carpet (left). Comparison to measured data (right). Flight 2, pass 1.

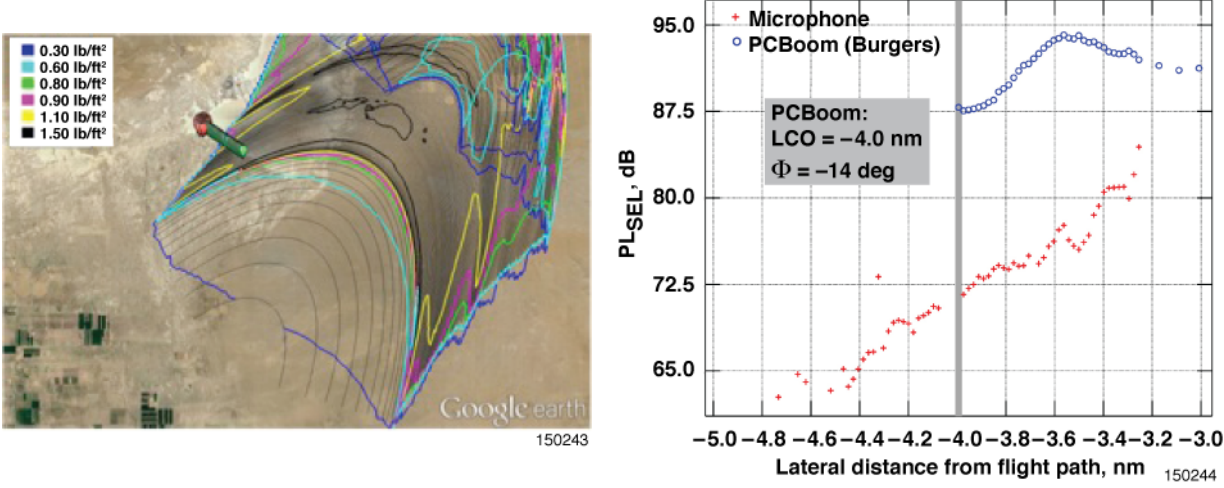


Figure 22. Predicted PCBoom sonic boom carpet (left). Comparison to measured data (right). Flight 4, pass 6.

Comparisons between PCBoom and real data near the lateral sonic boom carpet edge have varying results, but each of the five cases have some common similarities that are evident in figures 21 and 22. First, the sonic boom carpet predicted by PCBoom is consistently narrower

than the acoustic lateral cutoff because it does not model the transition zone or beyond. Microphones consistently showed evidence of notable noise levels present 1 – 2 nm beyond where the PCBoom solutions ended. Secondly, PCBoom shows a significant PL_{SEL} spike and complex focusing at the carpet edge when the airplane is modeled as accelerating (fig. 21). The modeled acceleration is evident by the increasing carpet width near the microphone array, and the spiking shows the complexity in the computer solution. Lastly, PL_{SEL} at the edge of the PCBoom solution were higher than the microphones for four out of the five cases.

Future Work and Considerations

While this paper presents an extensive amount of analysis and data for sonic boom lateral cutoff research, there are additional studies yet to be extracted from the FaINT effort. The FaINT provided a database to validate analytical studies into the lateral cutoff phenomenon. For example, Coulouvrat attempted to analytically describe various properties at the lateral cutoff, including the effects of crosswinds (ref. 7). The FaINT database can be used to validate studies such as these and to validate computer codes designed to model shadow zone acoustics, like LNTE (ref. 10). The FaINT also created a large database of sonic booms near the lateral cutoff measured by a phased, spiral, microphone array. That database can be used to perform beamforming analysis. It might be possible to use beamforming to image the acoustic sources and propagation path of sonic booms. In addition to the 37 FaINT lateral cutoff test points, 36 test points were also performed with the intent to study shadow side acoustics due to Mach cutoff. For given atmospheric conditions and flight altitude, there exists a threshold Mach number such that complete shock wave refraction (Mach cutoff) will occur at or above the ground. Below the altitude of complete refraction exists a shadow zone with evanescent waves.

Beyond the future work made possible by the FaINT data set, the research effort stimulated considerations for additional, related research. For each of the FaINT flights, the microphone arrays were located upwind of the aircraft. Future efforts may consider a similar array downwind of the aircraft to study the effects of crosswinds. Incorporating elevated microphones into the microphone array will add a vertical component to the measurements, which may provide additional knowledge about the directionality and elevation in the transition region. Performing a lateral cutoff test with varying strengths of temperature inversion may further validate the correlation between temperature inversions and acoustic level profiles in the transition region discussed in this paper.

Conclusions

Analysis of the FaINT lateral cutoff data produced several notable results. PL_{SEL} has been suggested as a metric for further study of sonic boom signatures of the type experienced in the lateral cutoff region. Sound exposure level metrics have been shown to be more consistent than other sonic boom metrics commonly used for studying N-waves, such as PL_{70} , L_{AF} , and L_{AS} .

Data suggests that sonic boom PL_{SEL} decreases in exponential fashion beyond the lateral cutoff. For well-behaved lateral sonic boom profiles, PL_{SEL} was shown to reach ambient noise at about 58.6 dB. Therefore, 65 dB PL_{SEL} (four times the ambient noise) is suggested to define the acoustic lateral cutoff of sonic booms produced during FaINT. Given this criterion, FaINT successfully placed the acoustic lateral cutoff on the microphone array 18 out of 37 times, which is respectable considering the threshold was not yet defined during planning, since data from the test itself was required to determine it.

The definition for the physical bounds of a sonic boom carpet is well known in the industry, defined as the lateral extent that sonic boom rays are able to intersect with the ground. This paper concludes that this definition is not adequate at describing the full acoustic envelope of a sonic boom. Computer codes are required to determine the extent of sonic boom ray propagation. Since

common, modern computer codes do not accurately model the transition region near the lateral cutoff, nor the shadow zone region beyond, however, those codes were shown to under represent the lateral area with notable noise due to sonic booms on the order of 1 - 2 nm.

The FaINT also demonstrated the ability to capture airborne midfield measurements of sonic booms near the carpet edge. Data collected at 4500 ft above the ground matched well with ground measurements, further validating the nature of a well-behaved lateral cutoff region. Airborne midfield measurements also suggested that the general lateral shape of an F-18 airplane sonic boom carpet might not be a simple bell-like shape within 2 – 3 nm of its flight path.

It was concluded that several factors affect sonic boom levels at the lateral cutoff. The most common factor during FaINT was atmospheric temperature inversions near the ground. These inversions sometimes resulted in PL_{SEL} values that were 15 dB higher than expected. This conclusion alone emphasizes the importance of understanding sonic boom carpet lateral cutoff phenomenon.

Lateral cutoff research is an important part of the continued effort to establish a commercial supersonic market. Examining acoustic propagation at the lateral edge of the sonic boom carpet will help the aerospace industry understand the full extent and ranges of noises generated by a supersonic aircraft. Such knowledge will mostly influence aircraft design, flight profile design, and airspace planning.

Appendix A – Spiral Microphone Array Description

Figure A1 shows an illustration of the spiral microphone array used during FaINT. The data from the secondary spiral array will be investigated in the future.

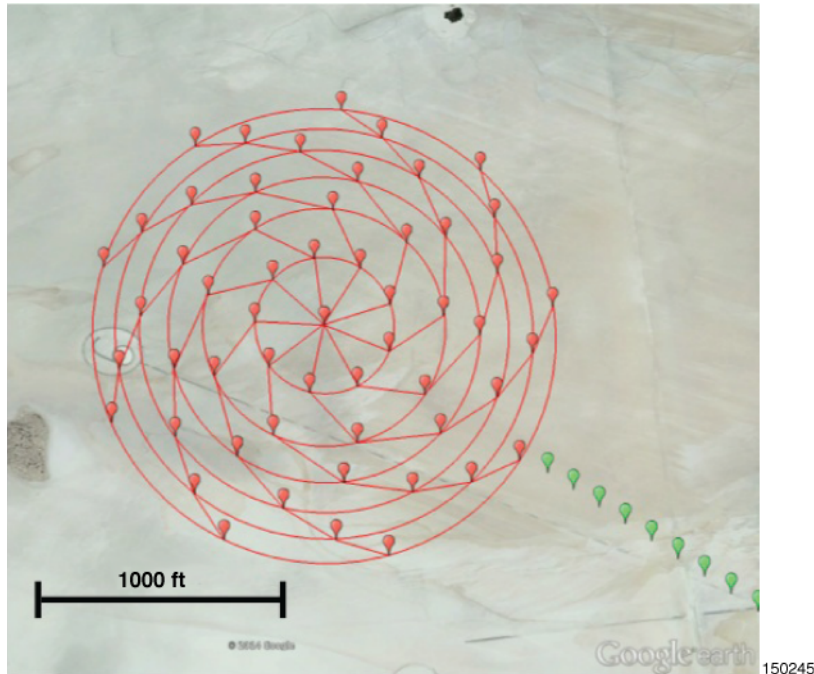


Figure A1. FaINT secondary/spiral microphone array.

The spiral array consisted of nine equally-spaced spiral arms with 55 discrete locations for microphones. Each spiral arm follows the polar equation:

$$r(\theta) = r_0 e^{\theta \cot(65\pi/180)} \quad (\text{Eq. 1(ref. 17)})$$

where the constant r_0 is 1 ft. One microphone location is at the center of the spiral, and where the nine spiral arms intersect, six radii of 300, 520, 675, 800, 900, and 1000 ft define the other 54 microphone locations. The radii were selected to achieve an equal aperture layout. Seven locations had a second microphone at the same location (to investigate variation due to microphone type) for a total of 62 microphones in the spiral array. The linear array microphone location closest to the spiral array was located 1125 ft from the center point.

For the spiral array, the primary microphones located at the center of the ground boards were all B&K 4192 microphones fitted onto B&K 2669C preamplifiers. For the seven locations with a second microphone, the second microphone, placed on the same ground board, was a B&K model 4193 with a low-frequency adapter fitted to the same type of B&K 2669C preamplifiers. It is understood that these microphones with the 2669C preamplifier do not have an appropriate low-frequency cutoff to faithfully reproduce a sonic boom signature, but they are sufficient for studying the direction of arrival. The secondary microphones were there for the purpose of studying the difference between the microphone types, and having a few microphones that could reproduce the sonic boom signature. Each of these 62 total microphones were connected to a B&K PULSE LAN-XI module located in one of four “field cases.” Due to the nearly 2000 ft diameter of the array, 31,500 ft of microphone cable was used. None of these exceeded 750 ft in length. The output of each B&K PULSE module is an Ethernet cable. Each field case contained an

Ethernet switch that was connected to all of the modules in that case. An additional port of the switch was a fiber optic connection. This was the long-haul connection for the field case back to the central data recording station. It required 4500 meters of single mode, fiber optic cable. These data were recorded at the central recording station using the B&K Labshop software. Also located in the central recording station was a TrueTime GPS synchronized clock. The output of this clock was IRIG-B timecode, which was connected to a LAN-XI module located in the central recording station. The four fiber optic network cables from the field cases, and the single copper network cable from the module in the central recording station, were all connected to a switch that was connected to the control and recording computer. Since the system supports Precision Time Protocol, this configuration resulted in all the sampled data being time synchronized to the sample and also stamped with GPS time.

Appendix B – Sound Metrics versus Lateral Cutoff Distance

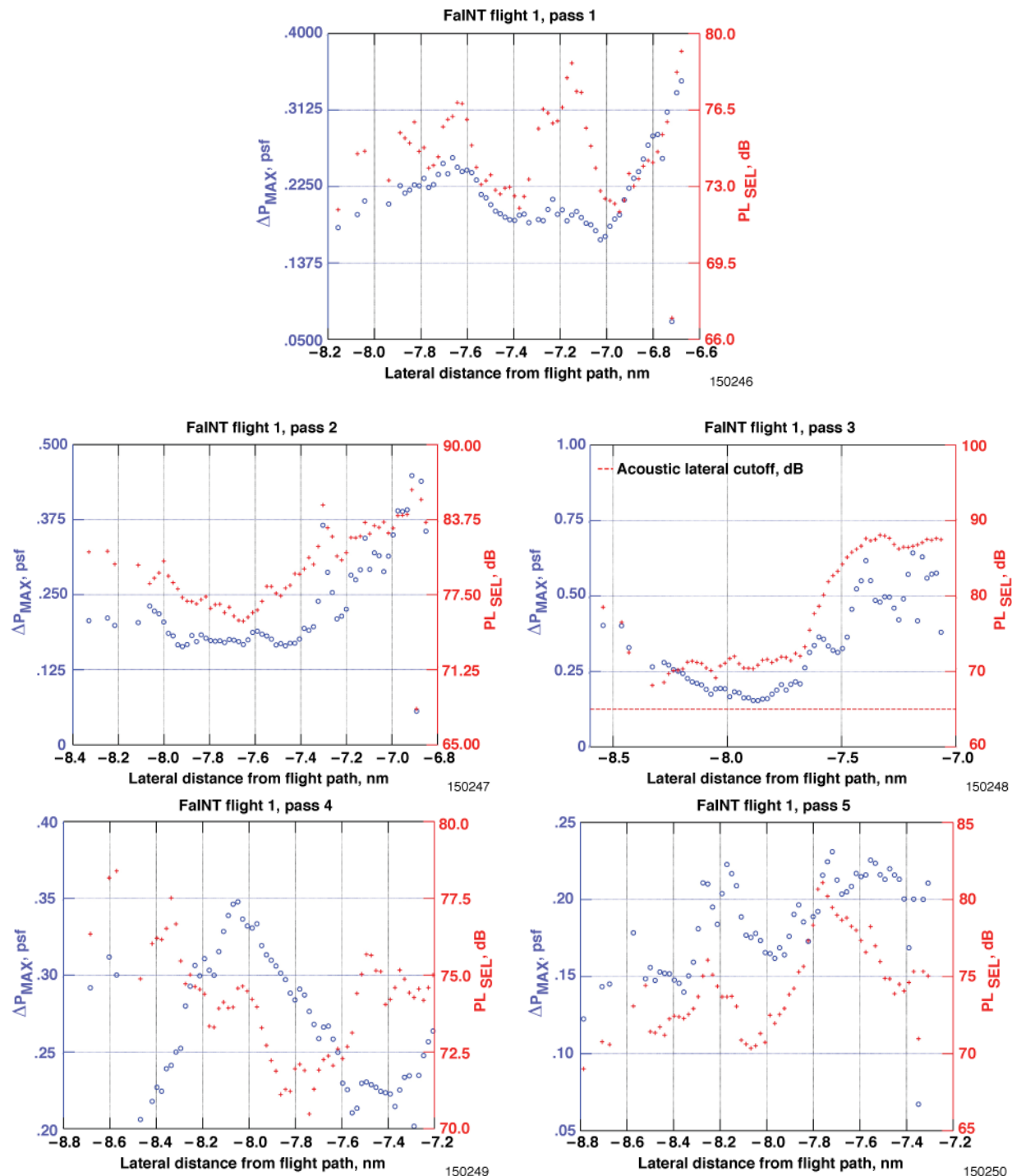


Figure B1. Lateral ground measurements. Flight 1.

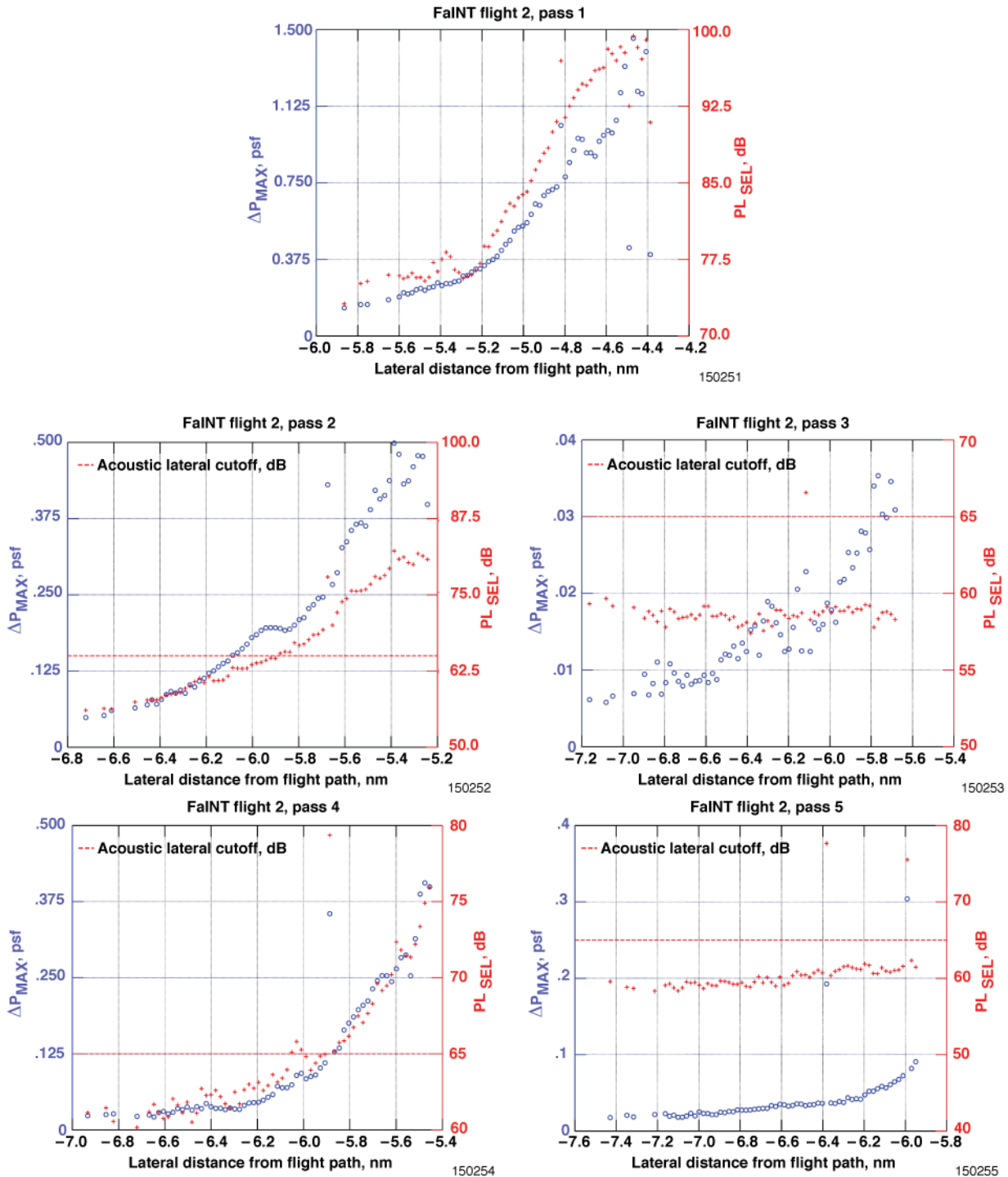


Figure B2. Lateral ground measurements. Flight 2.

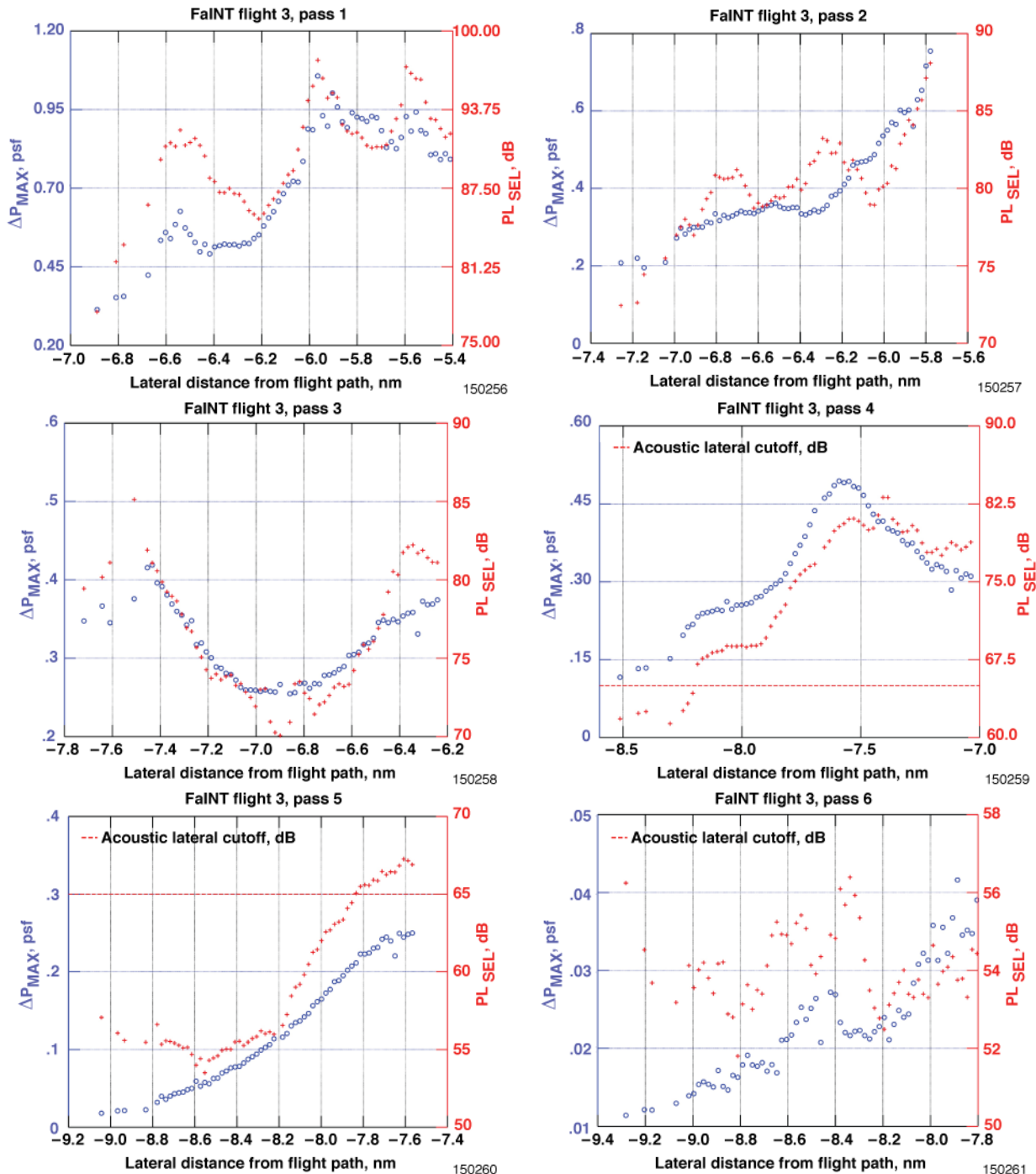


Figure B3. Lateral ground measurements. Flight 3.

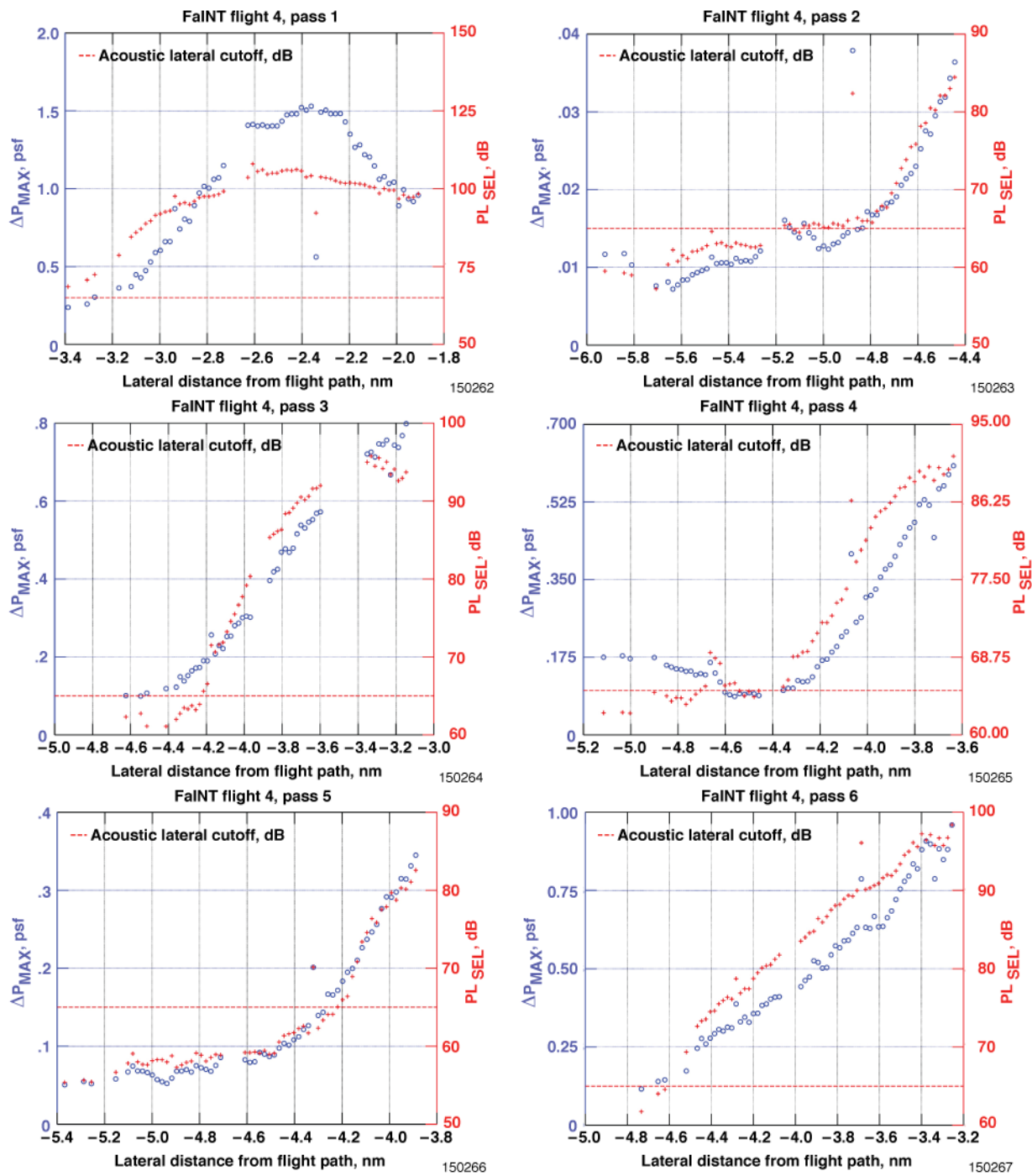


Figure B4. Lateral ground measurements. Flight 4.

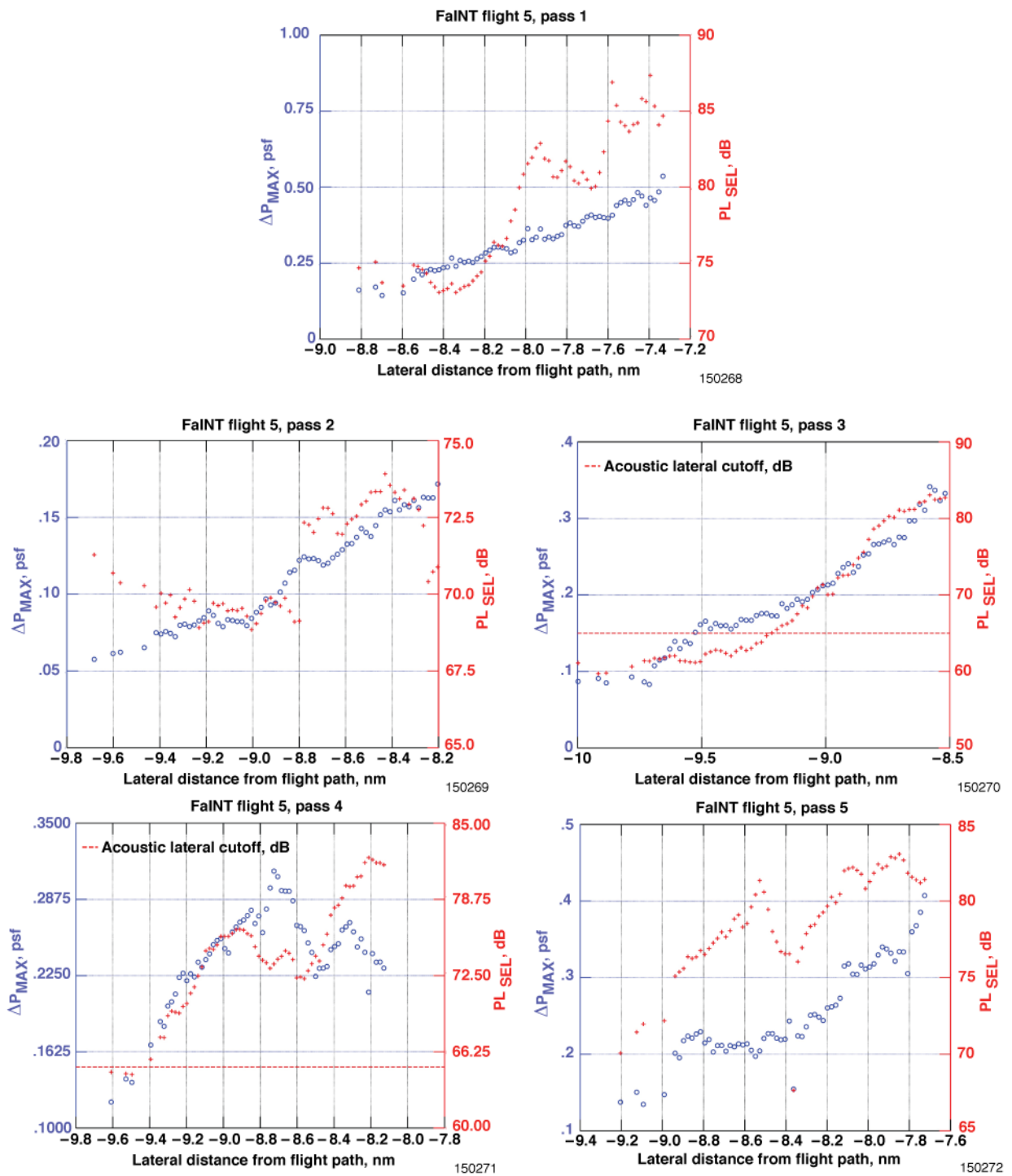


Figure B5. Lateral ground measurements. Flight 5.

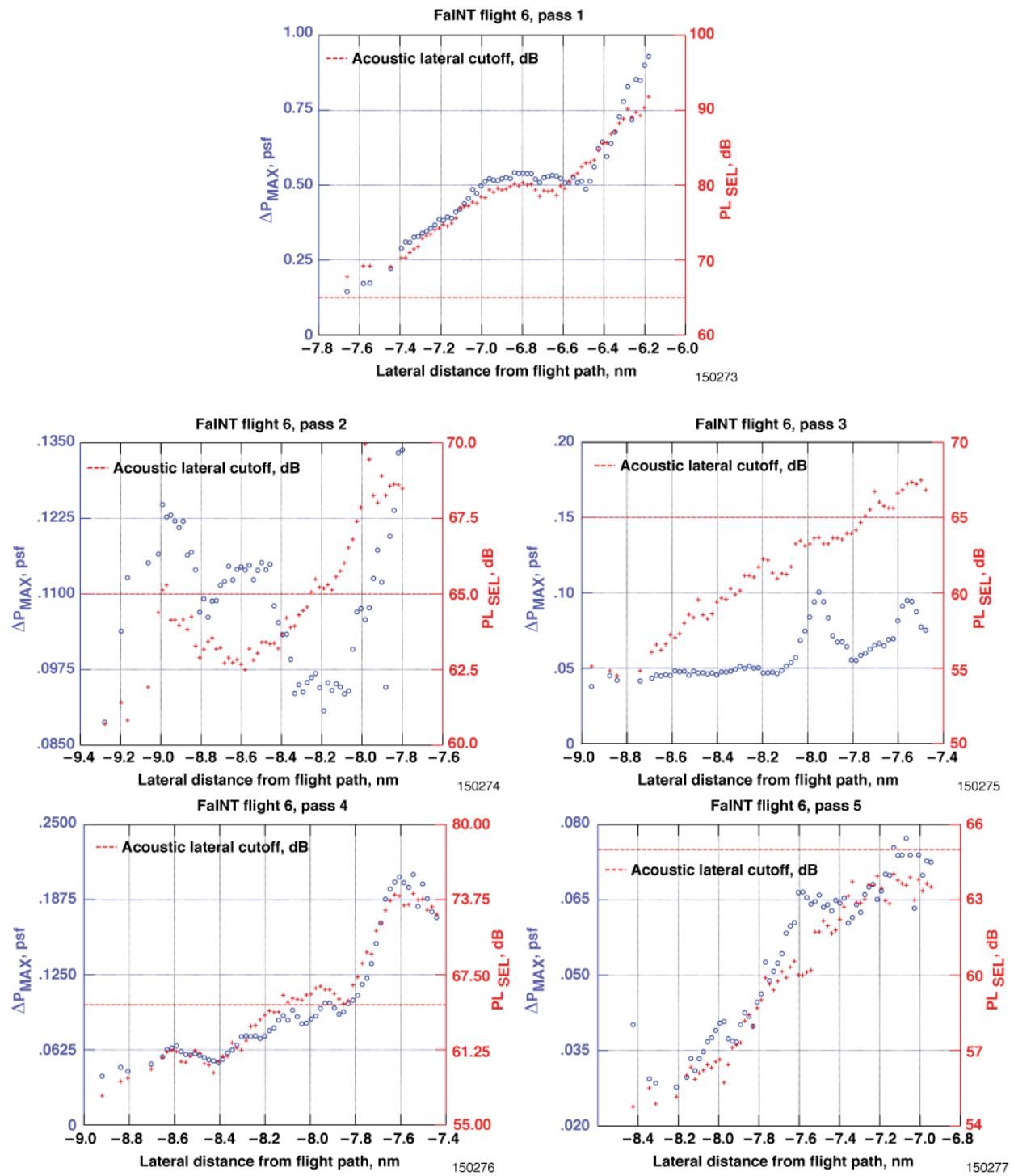


Figure B6. Lateral ground measurements. Flight 6.

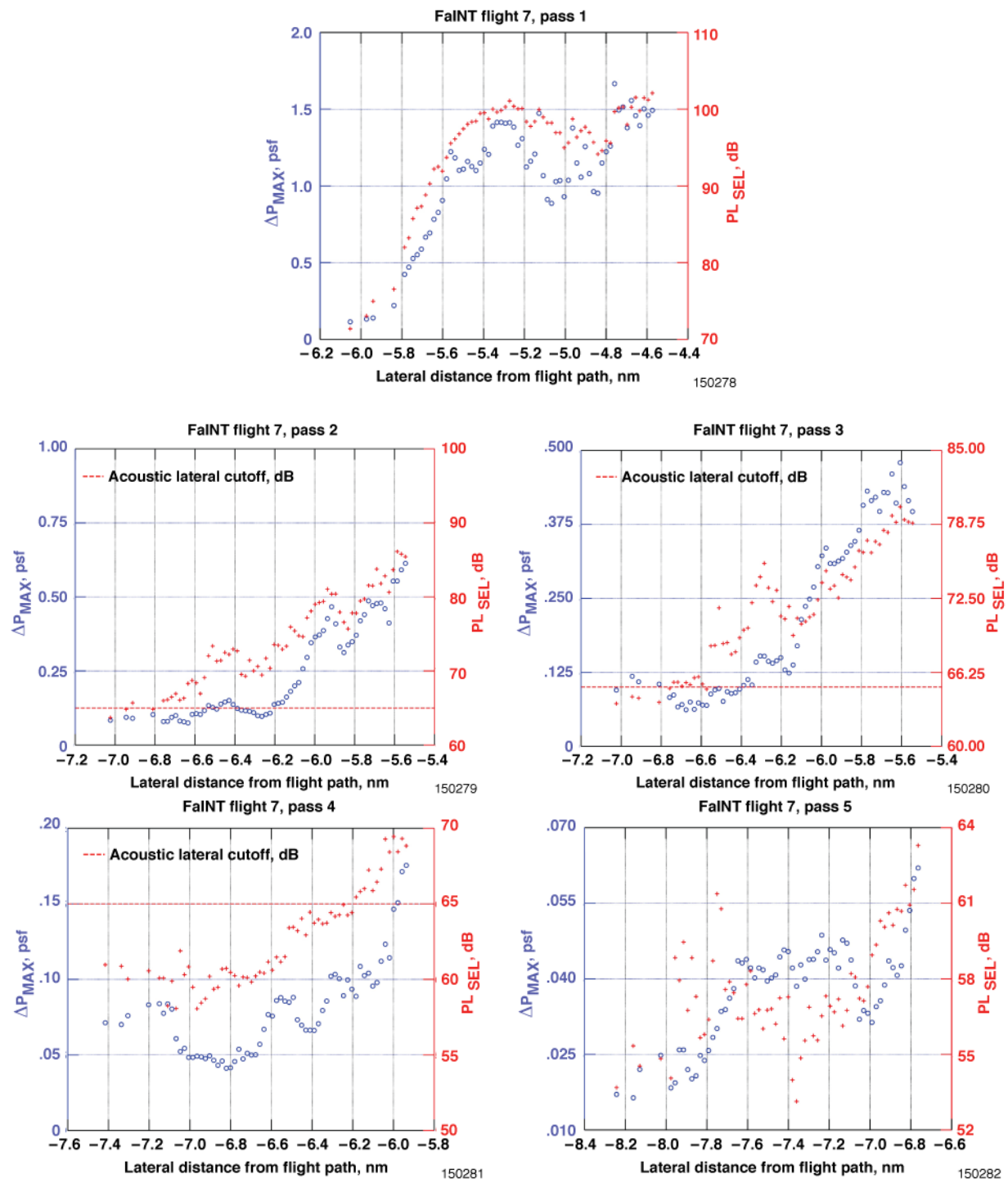


Figure B7. Lateral ground measurements. Flight 7.

Appendix C – Midfield Lateral Measurements

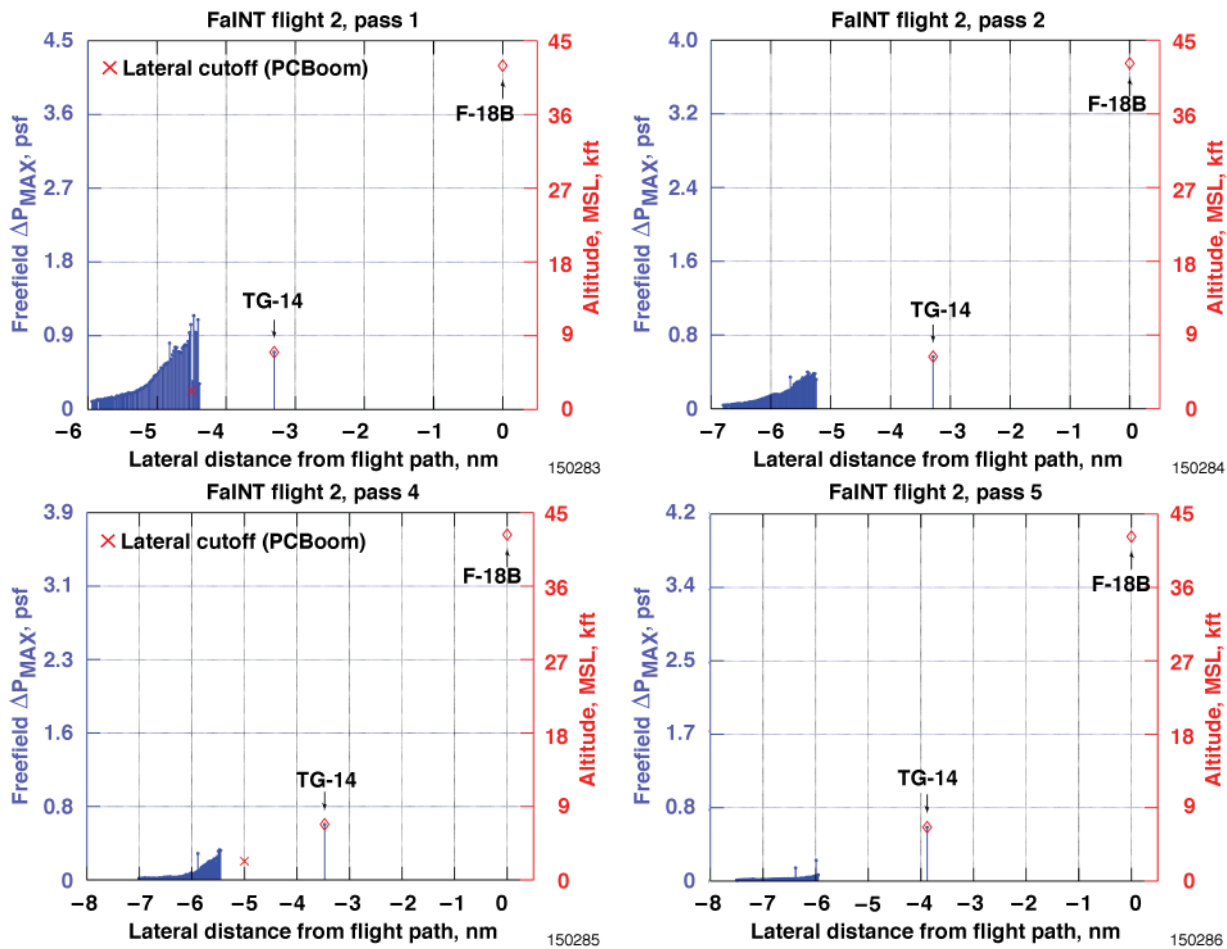


Figure C1. Midfield lateral measurements. Flight 2.

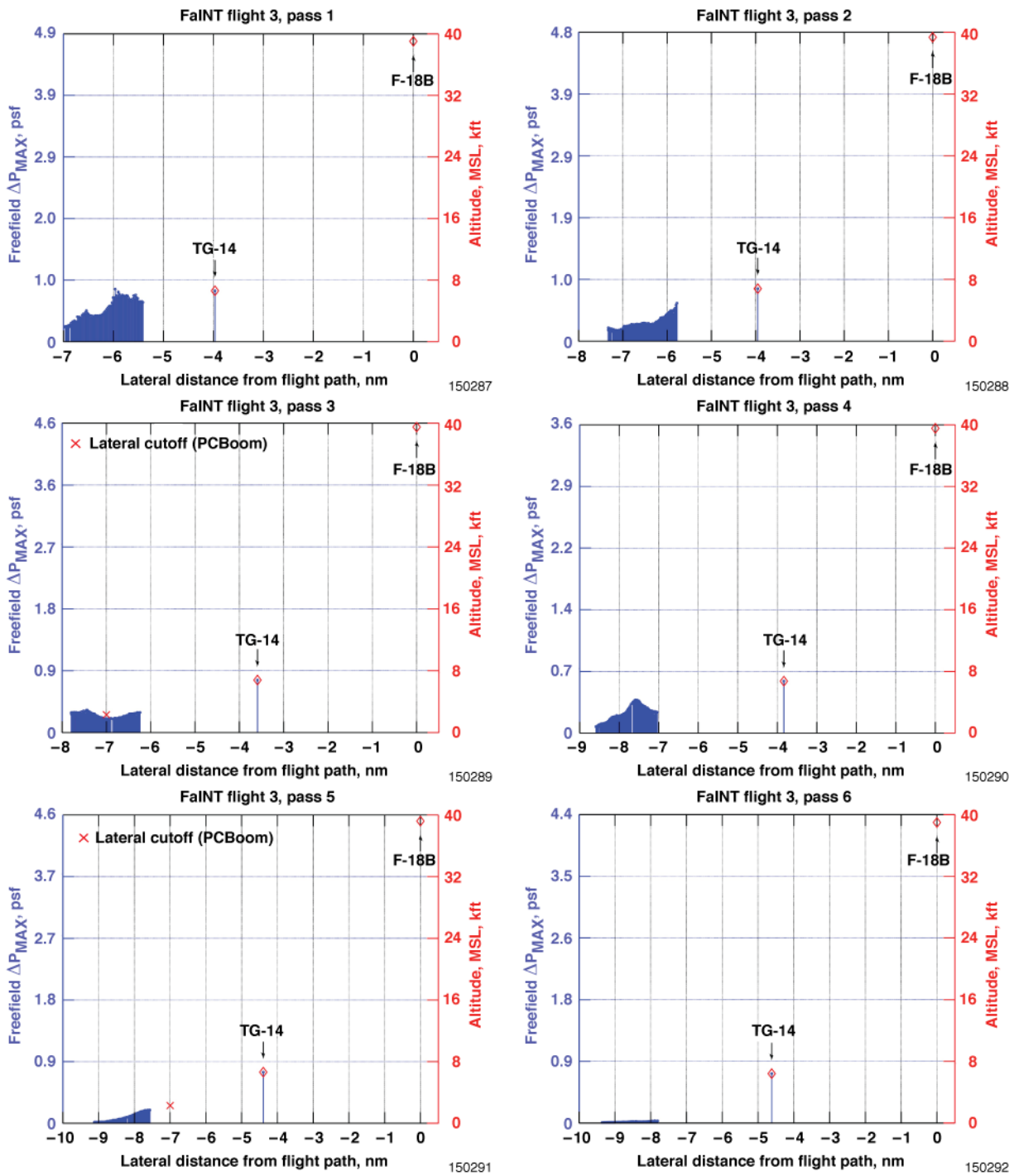


Figure C2. Midfield lateral measurements. Flight 3.

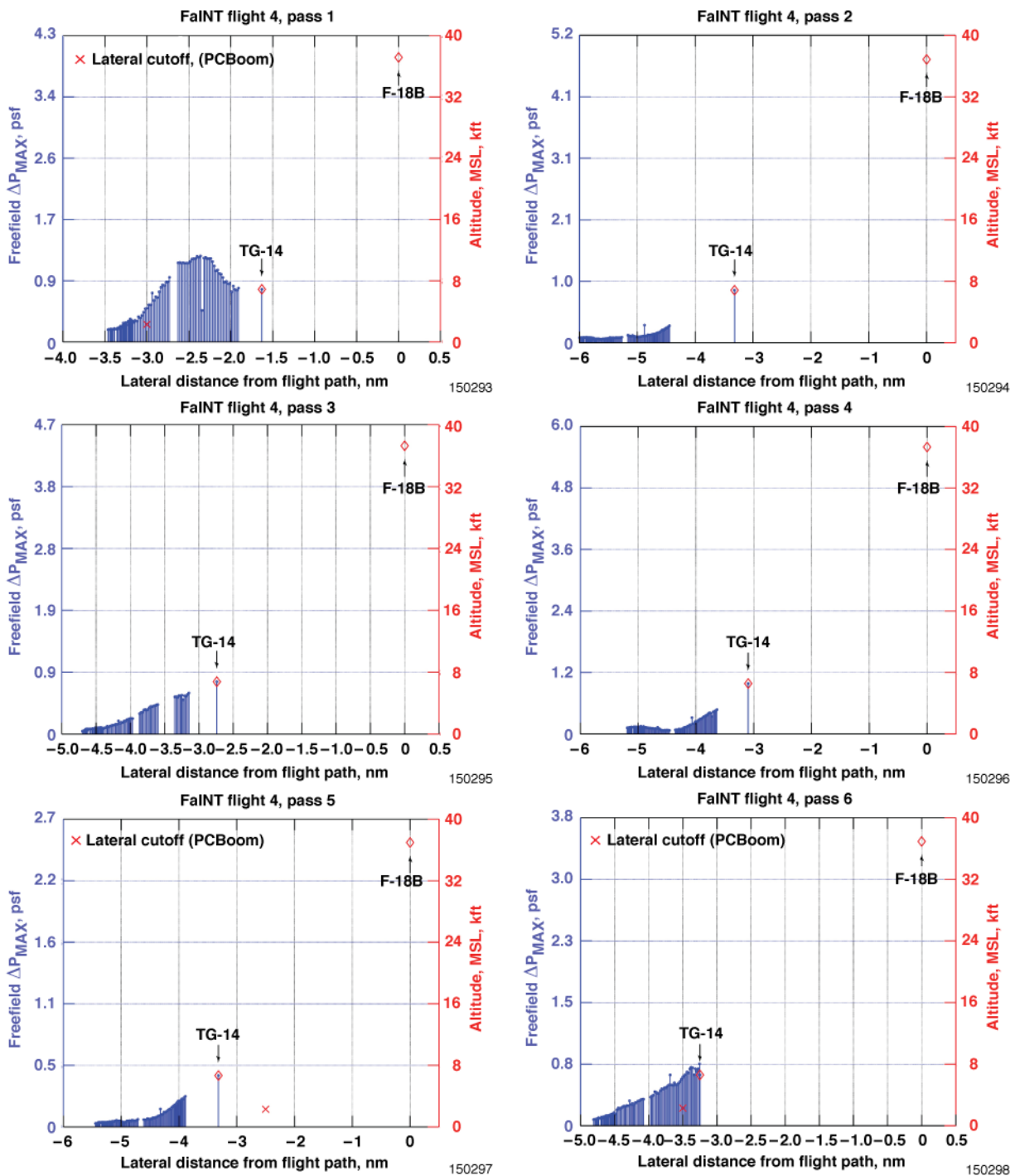


Figure C3. Midfield lateral measurements. Flight 4.

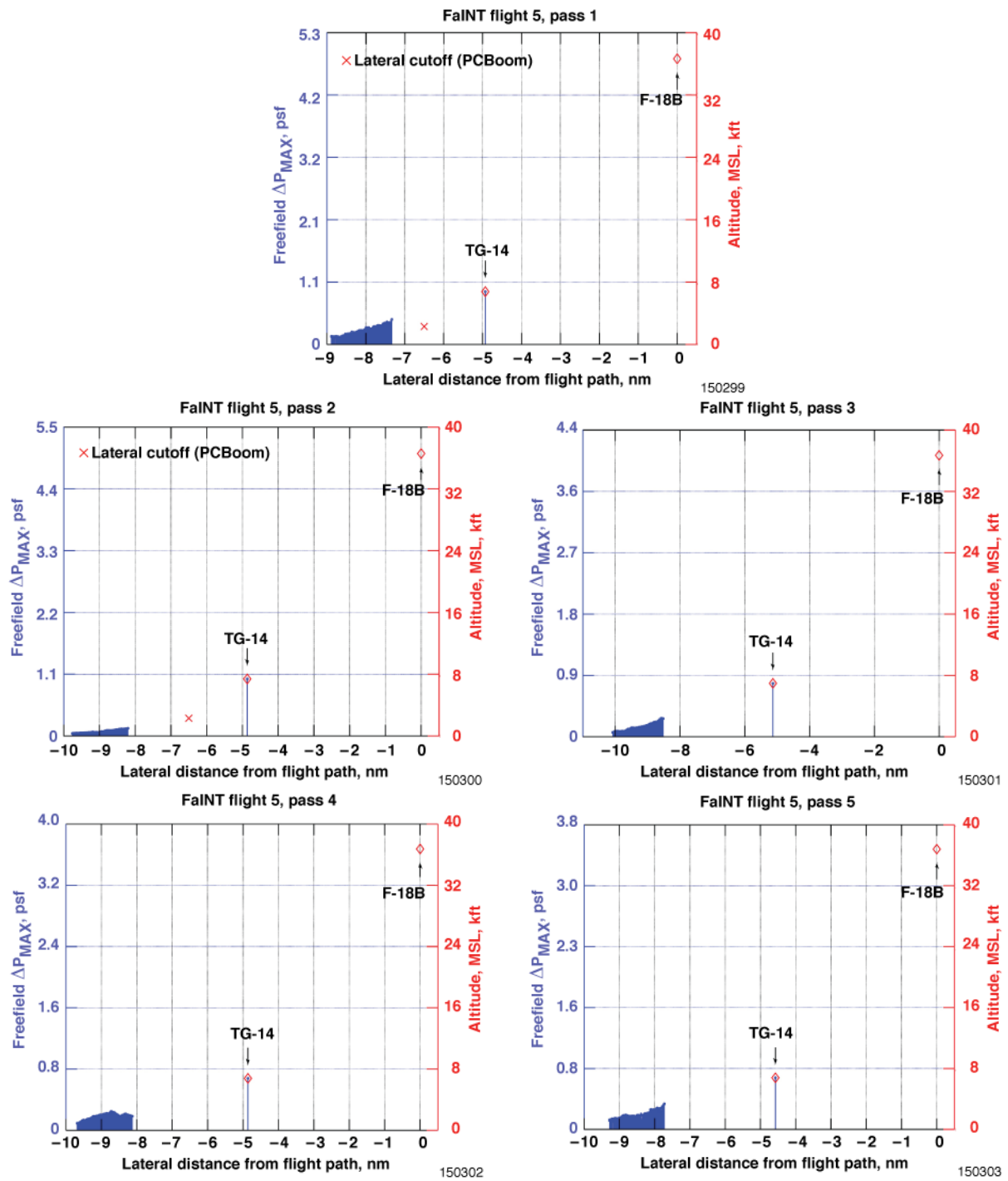


Figure C4. Midfield lateral measurements. Flight 5.

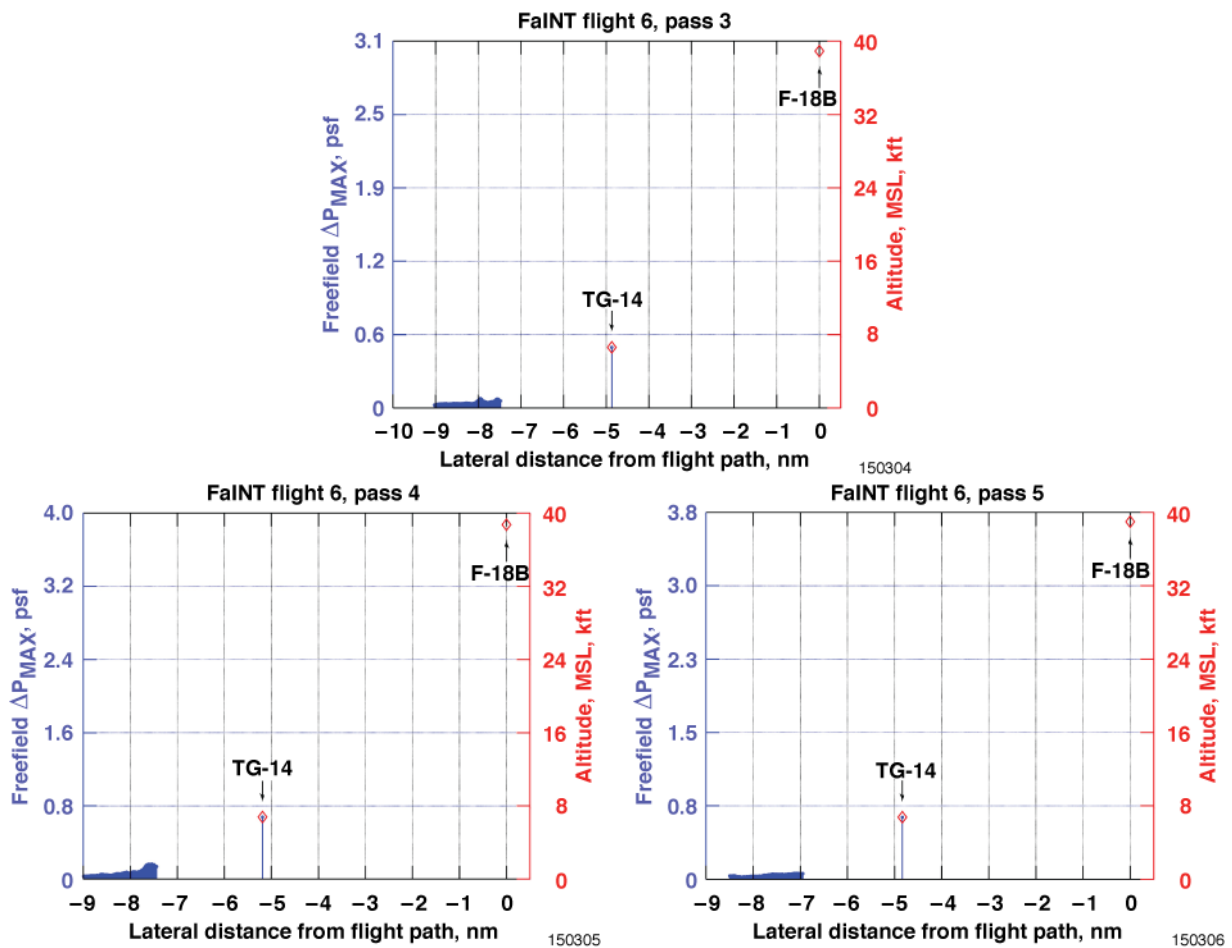


Figure C5. Midfield lateral measurements. Flight 6.

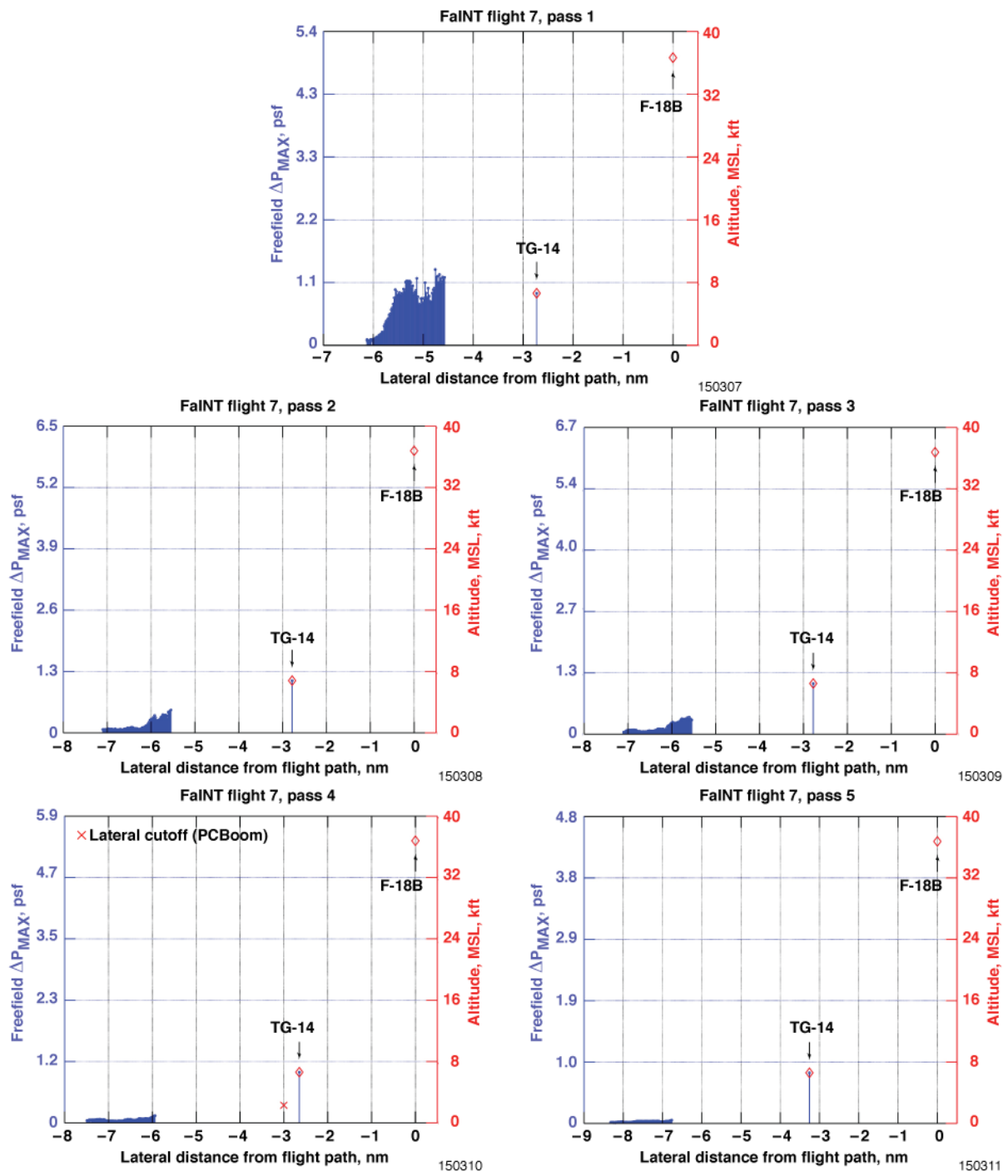


Figure C6. Midfield lateral measurements. Flight 7.

References

1. Page, Juliette A., Kenneth J. Plotkin, and Clif Wilmer, *PCBoom Version 6 Technical Reference and User Manual*, Wyle Report WR 09–20, Wyle Laboratories Inc., El Segundo, CA, 2009.
2. “U.S. Standard Atmosphere, 1976,” National Aeronautics and Space Administration, NASA-TM-X-74335.
3. Coulouvre, François. “Sonic boom in the shadow zone: A geometrical theory of diffraction,” Laboratoire de Modélisation en Mécanique, Université Pierre et Marie Curie, March 2001.
4. Darden, Christine M., Clemens A. Powell, Wallace D. Hayes, Albert R. George, and Allan D. Pierce, *Status of Sonic Boom Methodology and Understanding*, NASA Conference Publication 3027, 1988.
5. Rickley, E.J., and A.D. Pierce, *Detection and Assessment of Secondary Sonic Booms in New England*, U.S. Department of Transportation, FAA-AEE-80-22, May 1980.
6. Maglieri, Domenic J., Percy J. Bobbitt, Kenneth J. Plotkin, Kevin P. Shepherd, Peter G. Coen, and David M. Richwine, “Sonic Boom: Six Decades of Research,” NASA/SP-2014-622, 2014.
7. Shepherd, Kevin P., and Brenda M. Sullivan, *A Loudness Calculation Procedure Applied to Shaped Sonic Booms*. Vol. 3134. National Aeronautics and Space Administration, Office of Management, Scientific and Technical Information Program, 1991.
8. Haglund, George T. and Edward J. Kane, “Flight Test Measurements and Analysis of Sonic Boom Phenomena Near the Shock Wave Extremity,” NASA CR-2167, 1973.
9. Downing, J. M., “Lateral Spread of Sonic Boom Measurements from US Air Force Boomfile Flight Tests,” NASA CP-3172, pgs. 117-135. 1992.
10. Salamone, Joseph A., Victor W. Sparrow, Kenneth J. Plotkin, and Robbie Cowart, “SCAMP: Solution of the Lossy Nonlinear Tricomi Equation for Sonic Boom Focusing,” AIAA 2013-0935, 2013.
11. Stevens, S. S., “Perceived Level of Noise by Mark VII and Decibels (E),” *Journal of the Acoustical Society of America*, 51 (2), pp. 575-601, 1972.
12. Brusniak, Leon, James R. Underbrink, and Robert W. Stoker, “Acoustic Imaging of Aircraft Noise Sources Using Large Aperture Phased Arrays,” AIAA-2006-2715, 2006.
13. Haering, Edward A., Jr., Larry J. Cliatt II, Thomas J. Bunce, Thomas B. Gabrielson, Victor W. Sparrow, and Lance L. Locey, “Initial Results from the Variable Intensity Sonic Boom Propagation Database,” AIAA-2008-3034, 2008.
14. Cliatt, Larry J. II, Edward A. Haering Jr., Thomas P. Jones, Erin R. Waggoner, Ashley K. Flattery, and Scott L. Wiley, “A Flight Research Overview of WSPR, a Pilot Project for Sonic Boom Community Response,” AIAA 2014-2268, 2014.
15. “Acoustics – Description, Measurement and Assessment of Environmental Noise,” ISO 1996-2, International Organization for Standards, 2007.

16. "American National Standard – Specification for Sound Level Meters," ANSI S1.4: Specifications for Sound Level Meters, Acoustical Society of America, 1983.
17. Mueller, Thomas J., et al., "Aeroacoustic Measurements," New York: Springer-Verlag Berlin Heidelberg, 2002.